

COHERENCE-INDUCED ENTANGLEMENT

A Dissertation

by

HAN XIONG

Submitted to the Office of Graduate Studies of
Texas A&M University
in partial fulfillment of the requirements for the degree of

DOCTOR OF PHILOSOPHY

May 2006

Major Subject: Physics

COHERENCE-INDUCED ENTANGLEMENT

A Dissertation

by

HAN XIONG

Submitted to the Office of Graduate Studies of
Texas A&M University
in partial fulfillment of the requirements for the degree of

DOCTOR OF PHILOSOPHY

Approved by:

Co-Chairs of Committee,	M. Suhail Zubairy
	Marlan O. Scully
Committee Members,	George R. Welch
	Goong Chen
Head of Department,	Edward Fry

May 2006

Major Subject: Physics

ABSTRACT

Coherence-Induced Entanglement. (May 2006)

Han Xiong, B.S., Peking University;

M.S., Chinese Academy of Sciences

Co-Chairs of Advisory Committee: Dr. M. Suhail Zubairy
Dr. Marlan O. Scully

Coherence and entanglement are the two key concepts that distinguish quantum mechanics from classical mechanics. Many novel phenomena occurring in the quantum world are due to these two “physical quantities”. They also play essential roles in quantum computation and quantum information. For example, coherence, which says that a quantum mechanical system could be in a superposition state, makes the quantum parallel computing scheme possible; and entanglement, which says that two quantum systems separated in space could be in an intervened state, is the key factor in various quantum teleportation algorithms.

We have studied entanglement generation in various systems. We found that with atomic coherence, entanglement could be generated between two thermal fields with arbitrarily high temperatures. We also found that temperature difference instead of the purity of state is essential for the entanglement generation between an atom and a thermal field. We discovered that correlated spontaneous emission lasers (CELs) could be used to generate bright entanglement laser beams. As a special case of CEL systems, we studied entanglement generation in Non-degenerate Optical Parametric Amplifiers (NOPAs). We performed the input-output calculations for a NOPA system and showed that the two output optical beams are still entangled. This justifies our

idea that CEL (or NOPA) systems can be used as an ideal entanglement source for various quantum information schemes. From an experimental point of view, we considered the effects of pumping fluctuations on entanglement generation in CEL and NOPA systems. We found that these fluctuations, especially the phase diffusion processes, in the pump laser would greatly reduce the entanglement generated in such systems.

To My Parents: Yanxiao Xiong and Duanpu Zhou

ACKNOWLEDGMENTS

This research is supported by the Air Force Office of Scientific Research, Air Force Research Laboratories (Rome, New York), DARPA-QuIST, and the TAMU Telecommunication and Informatics Task Force (TITF) initiative.

Many thanks to my advisors Dr. M. Suhail Zubairy and Dr. Marlan O. Scully for all the time they have spent on me and all their help, patience, advising and instructions on my research and on my routine life. I also want to thank Dr. Fuli Li for his cooperation on the work in the first chapter; thanks to Dr. Julio Gea-Banacloche for his cooperation on the input-output problem for the NOPA system and thank Dr. Shahid Qamar for his cooperation in the effects of pumping noise in the entanglement amplifier problem. Many thanks to Mr. Clayton and Ms. Kim for helping me on all the stuff in this group. To all the members in the Institute of Quantum Studies group, including those friends who have left and those friends who are still here, I thank you for your friendship and your help.

I am proud to be a member of this wonderful group and I am proud to be an Aggie here. My wish for all of you is that you have a wonderful and fruitful future.

TABLE OF CONTENTS

CHAPTER		Page
I	INTRODUCTION	1
II	COHERENCE INDUCED ENTANGLEMENT	6
	A. Temperature difference induced entanglement	6
	1. The Jaynes-Cummings Model (JCM)	7
	2. Entanglement criterion	9
	3. Temperature difference as an important role in en- tanglement creation	11
	4. Control of entanglement creation	14
	B. Coherence induced entanglement	18
	1. System description and the Hamiltonian	18
	2. Entanglement generation via atomic coherence	20
III	CORRELATED SPONTANEOUS EMISSION LASER AS ENTANGLEMENT SOURCES	31
	A. Correlated spontaneous emission laser as an entangle- ment amplifier	31
	1. System description and the Hamiltonian	32
	2. Master equation	35
	3. Entanglement generation	39
	B. Entanglement generation in quantum beat lasers	44
	1. The entanglement criterion	45
	2. Entanglement production of non-degenerate para- metric converters	47
	3. Field entanglement in a quantum beat laser	49
IV	NON-DEGENERATE PARAMETRIC AMPLIFIER AS AN ENTANGLEMENT SOURCE	55
	A. The entanglement of an NOPA: below and above the threshold	55
	1. System description and the Hamiltonian	55
	2. Input and output calculations: below the threshold	57
	3. Input and output calculations: above the threshold	64

CHAPTER	Page
B. Effects of pump fluctuations on the entanglement of a NOPA system	70
1. Statistical description of the pump fluctuations	70
2. Entanglement measures	72
3. Phase diffusion upon entanglement generation	73
4. Effect of amplitude fluctuations	75
V SUMMARY	80
REFERENCES	81
VITA	87

LIST OF TABLES

TABLE		Page
I	Solutions of inequality (2.16)	14

LIST OF FIGURES

FIGURE		Page
1	Atomic coherence for a two-level atom	1
2	A Hanle effect CEL system	2
3	The Jaynes-Cummings interaction system	7
4	Entanglement dependance on time for different temperature of atoms. $\gamma_f = -0.01$ and $\langle n \rangle = 100$ for the thermal field	15
5	Entanglement dependance on the passage time of the atom through the classical field, $\Omega\tau = \pi/2.0$, (a) $\langle n \rangle = 0.3$; (b) $\langle n \rangle = 0.5$	17
6	A three-level atom in “V” configuration with initial populations $\rho_{aa}, \rho_{bb}, \rho_{cc}$ is prepared in a superpostion of upper level $ a\rangle$ and $ b\rangle$ by a resonant classical field. The atom then passes through a doubly resonant cavity which is resonant with $ a\rangle - c\rangle$ and $ b\rangle - c\rangle$ transitions. The fields inside the cavity are initially diagonal, such as a thermal state.	19
7	The solid lines are for the case with $\langle n_1 \rangle = 0.1$ and $\langle n_2 \rangle = 5.0$. The dashed lines are for the case with $\langle n_1 \rangle = 0.1$ and $\langle n_2 \rangle = 1.0$. gt=11.0.	27
8	The solid lines are for the case with $\langle n_1 \rangle = \langle n_2 \rangle = 1.0$. The dashed line is for the case with $T \rightarrow \infty$. gt=5.0 and $\rho_{aa} = 1$	28
9	The time evolution of the entanglement measurement with $\langle n_1 \rangle =$ 0.1, $\langle n_2 \rangle = 5.0$, and $\Omega\tau = \pi/4$	30
10	The time evolution of the entanglement measurement with $\langle n_1 \rangle =$ 1.0, $\langle n_2 \rangle = 1.0$, and $\Omega\tau = \pi/4$ and $\rho_{aa} = 1$	30

FIGURE

Page

11	(a) Schematics for the entanglement amplifier. Atomic medium is placed inside a doubly resonant cavity. (b) A three-level atomic system in a cascade configuration. The transitions between levels $ a\rangle - b\rangle$ and levels $ b\rangle - c\rangle$ at frequencies ν_1 and ν_2 are resonant with the cavity. The transition $ a\rangle - c\rangle$ is dipole forbidden and can be induced by strong magnetic fields. (c) A Raman three-level atomic system where the fields of frequencies ν_3 and ν_4 are strong classical driving fields and the the fields at frequencies ν_1 and ν_2 are resonant with the cavity modes.	33
12	(a) Time development of $(\Delta\hat{u})^2 + (\Delta\hat{v})^2$, and (b) $\langle\hat{N}\rangle$ for initial coherent states $ 100, -100\rangle$ in terms of the normalized time gt . Various parameters are $r_a = 22kHz$, $g = g_1 = g_2 = 43kHz$, $\kappa = \kappa_1 = \kappa_2 = 3.85kHz$, $\gamma = 20kHz$, $\Omega = 400kHz$. In these figures, 1 and 2 represent the results for the parametric case and the general case, respectively. Parameters are chosen such that they correspond to the micromaser experiments [64].	40
13	(a) Time development of $(\Delta\hat{u})^2 + (\Delta\hat{v})^2$ and (b) $\langle\hat{N}\rangle$ for initial vacuum states for the two modes with $\Omega/\gamma = 20, 23, 25$. Curves in (b) are truncated when $(\Delta\hat{u})^2 + (\Delta\hat{v})^2 = 2$ and the state is not necessarily entangled. The chosen parameters are $r_a = g = \gamma$ and $\kappa/g = 0.001$	41
14	The entanglement(a) and photon numbers(b) (the dash line is for mode 1 and the solid line is for mode 2) of a parametric quantum beat oscillator, we take $\epsilon = 1$ and the initial state of the field being $ 10, 0\rangle$ for a special case.	48
15	A schematic of the system setup for a quantum beat laser	50
16	The time evolution of entanglement(a) and photon numbers(b)(the dash line is for mode 1 and the solid line is for mode 2) of a quantum beat laser. The following parameters have been chosen: $r_a = 1$, $\Omega = 10$, $\gamma = 0.1$, $g = 1$, $\Delta = 0$ and $\phi = \pi$	53

FIGURE

Page

17	A scheme for our non-degenerate parametric oscillator system. It consists of a type II crystal located in an optical cavity tuned to allow three modes of the light field of frequencies ω_1 , ω_2 and ω_3 with $\omega_1 + \omega_2 = \omega_3$. Mode 3 is pumped by an external laser at frequency ω_3 . Modes 1 and 2 are the signal and idler modes of this oscillator that interact with two baths (bath 1 and bath 2), with $a_{in}(b_{in})$ and $a_{out}(b_{out})$ to be the input and output fields of bath 1 (bath 2).	56
18	Dependences of spectrum of the quantum fluctuations of EPR-like operators and intensities on the dimensionless frequency shift ω/γ , for system operating below the threshold $ \epsilon/\gamma = 0.1$	63
19	Dependences of spectrum of the quantum fluctuations of EPR-like operators and intensities on the dimensionless frequency shift ω/γ , for system operating above the threshold $ E = 2 E _{thres} = 2\frac{\gamma_3}{2g}$, with $g/\gamma = 1$ and $\gamma_3/\gamma = 10$	69
20	$(\Delta\hat{u})^2 + (\Delta\hat{v})^2$ vs $\beta_0 t$ for $D/\beta_0 = 0.0, 0.01$, and 0.10	76
21	$(\Delta\hat{u})^2 + (\Delta\hat{v})^2$ vs $\beta_0 t$ for no noise; $I_A/\beta_0 = 0.5$, $\Gamma/\beta_0 = 0.5$; $I_A/\beta_0 = 0.5$, $\Gamma/\beta_0 = 1.0$	78

CHAPTER I

INTRODUCTION

When coherent electromagnetic fields interact with multi-level atomic systems, coherence between levels may be induced. This state of the atom is called atomic coherence. A simple example of atomic coherence (see Fig. 1 for a better viewing) would be a two-level atom with the ground state $|b\rangle$ and excited state $|a\rangle$. If the atom is in a superposition state $|\phi\rangle = c_b|b\rangle + c_a|a\rangle$ and c_b, c_a are non-zero complex amplitudes, we then say that the atom has atomic coherence. This look-like simple state is actually very counterintuitive to our classical common sense and cannot be interpreted classically. Especially, we no longer say that the atom is in state ‘ $|b\rangle$ ’ or ‘ $|a\rangle$ ’, instead we say that the atom is in state ‘ $|b\rangle$ and $|a\rangle$ ’ simultaneously.

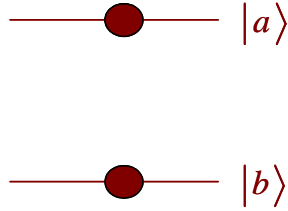


Fig. 1. Atomic coherence for a two-level atom

Atomic coherence has put a great impact on all areas of physics and is continuously to be an attractive research area. For example, Scully *et. al.* showed that given a small amount of atomic coherence, one could extract work from a single heat bath, although the deep physics behind the second law of thermodynamics is still not violated [1]. Other novel phenomena induced by atomic coherence include corre-

[†]The journal model is *Physical Review A*.

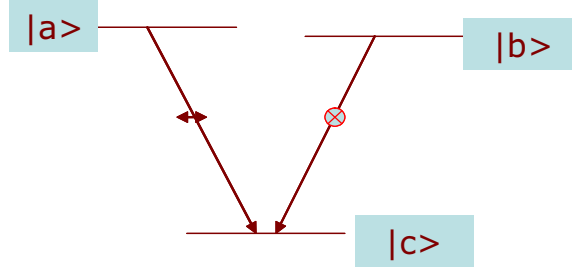


Fig. 2. A Hanle effect CEL system

lated spontaneous emission lasers (CELs) [2, 3, 4, 5, 6, 7], refractive index enhancement [8], coherent population trapping [9], electromagnetically induced transparency (EIT) [10], lasing without inversion (LWI) [11, 12, 13], etc.

Take Hanle effect correlated emission laser (one type of CEL) as an example, It consists of a laser medium with three-level atoms and a doubly resonant cavity (Fig. 2). The two upper levels of the three-level atoms are the ‘linear polarization’ states formed from a single ‘elliptical polarization’ state. The two transitions $|a\rangle \leftrightarrow |c\rangle$ and $|b\rangle \leftrightarrow |c\rangle$ drive the two cavity modes, which forms two quantum paths in this system. When the upper level $|a\rangle$ and $|b\rangle$ are prepared in a coherent superposition, these two paths are strongly correlated so that the diffusion of the relative phase angle between the two linearly polarized cavity modes caused by spontaneous fluctuations can be highly suppressed. We will discuss CEL systems again in Chapter III.

Whatever happened to one particle would thus immediately affect the other particle, wherever in the universe it may be. Einstein called this “Spooky action at a distance.”

Amir D. Aczel, Entanglement, The Greatest Mystery In Physics

The most mysterious phenomenon in quantum mechanics is called entanglement. The idea of quantum entanglement is first inferred by Einstein, Podolsky and Rosen

(generally referred as EPR). In their famous 1935 paper [14] on the Physical Review, EPR proposed a gedanken experiment which showed that both position and momentum variables could be simultaneously assigned to a single localized particle with certainty (physical reality) if two particles are initially prepared in the ideal position and momentum correlated state (entangled state). By locality, EPR means that a measurement performed on one of two systems which are spatially separated and without interaction cannot disturb another one. EPR argued that if assuming locality as a commonly accepted fact, their results violates the principle of quantum mechanics that two physical quantities represented by two noncommutable operators (for example, the position and momentum operators) can not simultaneously have the same reality. They therefore argued that quantum mechanics was incomplete. Later on, Shrödinger extended the work of EPR and give the name to “Entanglement” [15]. Many works have been done following the line of EPR on quantum entanglement. Bohm proposed a new and simpler version of EPR arguement for discrete variables such as spins [16]. John Bell discovered his famous inequality, which can be used to verify quantum mechanics or local version of hidden variable theories [17] etc.. In combination of information theory with quantum mechanics, a new branch of research what we now collectively called “Quantum Information Science” has been borned; and quantum entanglement is a seed to this birth.

The generation of entangled states have been experimentally investigated in various systems from atoms, ions, photons and quadrature-phase amplitudes of the electromagnetic field. In 1997, Hagley *et. al.*[18] produced the atomic entangled state in which two atoms are in two different circular Rydberg states and separated by a distance of the order of 1 cm. Turchette *et. al.*[19] showed that the internal states of two trapped ions can be prepared in both the Bell-like singlet and triplet entangled states in a deterministic fashion. Along the lines of the proposal suggested by

Molmer and Sorensen[20], Sackett[21] *et. al.* realized experimentally entangled states of four trapped ions. Based on Duan *et. al.*'s proposal[22], Julsgaard *et. al.* [23] demonstrated experimentally at the level of macroscopical entanglement between two separate samples of atoms each of which contains 10^{12} atoms. As for the generation of entangled states of photons, a great progress has been made in recent years. Using a single circular Rydberg atom, Rauschenbeutel *et. al.*[24] prepared two modes of a superconducting cavity in a maximally entangled state in which the two modes share a single photon. In most EPR optical experiments, pairs of polarization photons flying apart can be created in an entangled state by either spontaneous emission cascade in an atom[25, 26, 27], or down-conversion in a nonlinear medium[28, 29]. Entangled states of three[30], four[31] and five photons[32] have been realized. For the purpose of application, an entangled state containing more photons become more interesting. Tsujino *et. al.*[33] showed the experimental generation of two-photon-polarization states by parametric down-conversion. Eisenberg *et. al.*[34] created a bipartite multiphoton entangled state through stimulated parametric down-conversion of strong laser pulses in a nonlinear crystal. Quantum information processes based on the entangled quadrature-phase amplitudes of the electromagnetic field show some advantages and the generation of the entangled quadrature-phase amplitudes of an optical field has attracted much attention[35] recently. In usual experiments, the entangled quadrature-phase optical beams are generated by two vacuum squeezed states via a beam splitter and are in a two-mode quadrature squeezed vacuum. In a recent experiment, Zhang *et. al.*[36] showed that the bright entangled signal and idler beams can be generated by a nondegenerate optical parametric amplifier.

Many algorithms and computation techniques in quantum information science have been based on quantum entanglement. It is the basis for emerging technologies such as quantum computing [37], quantum superdense coding[38] and quantum

cryptography [39]. It has also been used for experiments in quantum teleportation [40, 41, 42]. Seeking for better entanglement sources has become an attractive goal for quantum information scientists.

We have considered various of crucial points for entanglement generations. Problems such as entanglement measure, decoherence effects, entanglement generation between thermal states and entanglement amplifiers etc. have been extensively studied in our research. This dissertation is a collective of several topics that we have completed in our research.

CHAPTER II

COHERENCE INDUCED ENTANGLEMENT

Atomic coherence and quantum entanglement are two different quantum concepts, however, they are sometimes closely related. In this chapter, we show their relation in an atom-field interaction system. But before that, I will deviate from our topic a little bit and talk about a very interesting system, which shows that temperature difference can produce entanglement between a two-level atom and a thermal field with an arbitrarily high temperature.

A. Temperature difference induced entanglement

In practice, entanglement of pure states is hard to maintain and produce due to the decoherence and other interactions with the environment. Thus, understanding and quantifying entanglement of mixed states becomes more and more interesting in recent researches [43, 44, 45, 46]. The most common mixed state may be a thermal state which represents a system in contact with a large reservoir with a specific temperature. An interesting problem is then the creation of entanglement in thermal states. In a recent paper, Bose and his colleagues have shown that entanglement could be produced in the interaction of a two-level atom initially prepared in a pure state with a thermal field with arbitrarily high temperature [47]. To fully understand this problem, a general discussion when the atom and the field are both initially in thermal states need to be addressed. We discuss this case in this section. We show that the temperature difference between the atom and the field is a very crucial factor and entanglement can be produced when the temperature difference is sufficiently large no matter how high the temperature of the atom and the field is. It is known in classical thermodynamics, temperature difference determines the heat exchange

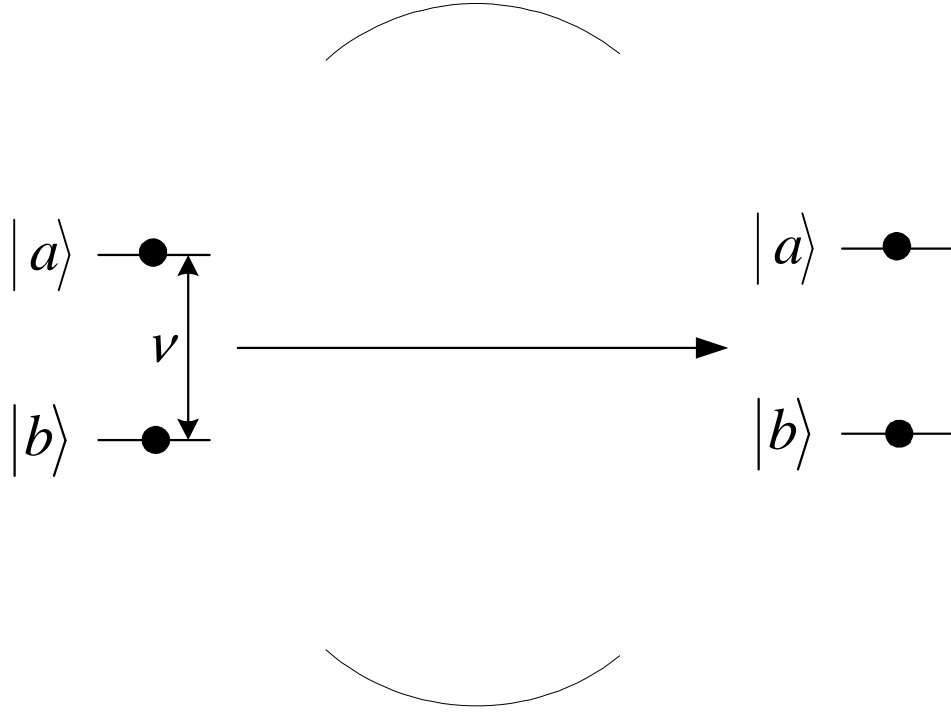


Fig. 3. The Jaynes-Cummings interaction system

rate, this then hints a sufficiently large amount of heat exchange is necessary for the creation of entanglement between a thermal atom and a thermal field. Generally, entanglement cannot be produced when the atom and the field are initially in thermal equilibrium. However, the thermal equilibrium can be deviated by applying a unitary transformation on the atom and the creation of entanglement will very much depend on the unitary transformation that we applied. This provides us a method by which we can control the entanglement of the whole system.

1. The Jaynes-Cummings Model (JCM)

We start from the Jaynes-Cummings Model (JCM) of the atom-field interaction [48]. This model describes the interaction of a two-level atom and a near resonant quantized

field as shown in Fig. 3. In the interaction picture and with the dipole and rotating wave approximations, the Hamiltonian of this system is [48]

$$\hat{H} = \hbar g(|a\rangle\langle b|\hat{a} + |b\rangle\langle a|\hat{a}^\dagger), \quad (2.1)$$

where \hat{a} and \hat{a}^\dagger are the destruction and creation operators of the field and g is the vacuum rabi frequency (We have assumed a resonant interaction here). The time evolution operator is

$$\begin{aligned} \hat{U}(t) &= e^{-\frac{i}{\hbar}\hat{H}t} \\ &= \cos(\sqrt{\hat{a}\hat{a}^\dagger}gt)|a\rangle\langle a| + \cos(\sqrt{\hat{a}^\dagger\hat{a}}gt)|b\rangle\langle b| \\ &\quad - i\hat{a}\frac{\sin(\sqrt{\hat{a}^\dagger\hat{a}}gt)}{\sqrt{\hat{a}^\dagger\hat{a}}}|a\rangle\langle b| - i\frac{\sin(\sqrt{\hat{a}\hat{a}^\dagger}gt)}{\sqrt{\hat{a}\hat{a}^\dagger}}\hat{a}^\dagger|b\rangle\langle a|. \end{aligned} \quad (2.2)$$

Suppose that the atom-field combined system is initially in a separable state

$$\hat{\rho}_{af}(0) = \sum_{n=0}^{\infty} P_n |n\rangle\langle n| \otimes (\rho_{aa}|a\rangle\langle a| + \rho_{bb}|b\rangle\langle b| + \rho_{ab}|a\rangle\langle b| + \rho_{ba}|b\rangle\langle a|), \quad (2.3)$$

where the field is assumed to be in a thermal state and the photon probability distribution P_n for number states $|n\rangle$ is given by

$$P_n = \frac{\langle n \rangle^n}{(1 + \langle n \rangle)^{n+1}}, \quad (2.4)$$

with $\langle n \rangle = (e^{\hbar\nu/k_B T_f} - 1)^{-1}$. Here, ν is the frequency of the field (for a resonant interaction $\nu = \omega_{ab}$), k_B is the Boltzman constant and T_f is the temperature of the field. By applying the time evolution operator (2.2) on the initial state (2.3), we obtain

$$\hat{\rho}_{af}(t) = \hat{U}(t)\hat{\rho}_{af}(0)\hat{U}^\dagger(t) = \sum_{n=0}^{\infty} P_n \hat{\rho}_{af}^n(t) \quad (2.5)$$

where,

$$\begin{aligned}
\hat{\rho}_{af}^n(t) = & \rho_{aa}[C_{n+1}^2|n, a\rangle\langle n, a| + S_{n+1}^2|n+1, b\rangle\langle n+1, b| \\
& + iS_{n+1}C_{n+1}(|n, a\rangle\langle n+1, b| - |n+1, b\rangle\langle n, a|)] \\
& + \rho_{bb}[C_n^2|n, b\rangle\langle n, b| + S_n^2|n-1, a\rangle\langle n-1, a| \\
& - iS_nC_n(|n-1, a\rangle\langle n, b| - |n, b\rangle\langle n-1, a|)] \\
& + \rho_{ba}[C_nC_{n+1}|n, b\rangle\langle n, a| + S_nS_{n+1}|n-1, a\rangle\langle n+1, b| \\
& - iS_nC_{n+1}|n-1, a\rangle\langle n, a| + iS_{n+1}C_n|n, b\rangle\langle n+1, b|] \\
& + \rho_{ab}[C_nC_{n+1}|n, a\rangle\langle n, b| + S_nS_{n+1}|n+1, b\rangle\langle n-1, a| \\
& - iS_{n+1}C_n|n+1, b\rangle\langle n, b| + iS_nC_{n+1}|n, a\rangle\langle n-1, a|],
\end{aligned} \tag{2.6}$$

with $C_n = \cos(\sqrt{n}gt)$ and $S_n = \sin(\sqrt{n}gt)$. This is the time evolution of the density operator of the atom-thermal field system.

2. Entanglement criterion

We use a sufficient entanglement criterion proposed by Peres et. al. [49] to estimate the entanglement between the atom and the field. It says that for a bipartite system if the partial transposed density matrix of a state has negative eigenvalues the state is entangled. This criterion has been proved to be a necessary and sufficient condition for 2x2 and 2x3 systems and Gaussian continuous variable states [50, 51]. However, we note that the state (2.5) is a infinite dimensional matrix. It is difficult if not impossible to calculate the eigenvalues for such matrices. To overcome this, we can first project the state (2.5) onto a subspace equivalent to a 2x2 system. For example, we can define the projection operators $\hat{W}_n (n = 0, 2, 4, \dots)$ which locally project the field state into a subspace spanned by $|n\rangle$ and $|n+1\rangle$ as

$$\hat{W}_n = |n\rangle\langle n| + |n+1\rangle\langle n+1|. \tag{2.7}$$

If one of them (for a specific n) is applied on the state (2.5), the outcome will be

$$\begin{aligned}
 (\hat{\rho}_{af})_n &= (I \otimes \hat{W}_n) \hat{\rho}_{af}(t) (I \otimes \hat{W}_n) \\
 &= \begin{pmatrix} \rho_{b,n;b,n} & \rho_{b,n;b,n+1} & \rho_{b,n;a,n} & 0 \\ \rho_{b,n+1;b,n} & \rho_{b,n+1;b,n+1} & \rho_{b,n+1;a,n} & \rho_{b,n+1;a,n+1} \\ \rho_{a,n;b,n} & \rho_{a,n;b,n+1} & \rho_{a,n;a,n} & \rho_{a,n;a,n+1} \\ 0 & \rho_{a,n+1;b,n+1} & \rho_{a,n+1;a,n} & \rho_{a,n+1;a,n+1} \end{pmatrix},
 \end{aligned}$$

where I is the identity operator on the atom subspace and these matrix elements are

$$\begin{aligned}
 \rho_{b,n;b,n} &= P_n \rho_{bb} C_n^2 + P_{n-1} \rho_{aa} S_n^2 \\
 \rho_{a,n;a,n} &= P_n \rho_{aa} C_{n+1}^2 + P_{n+1} \rho_{bb} S_{n+1}^2 \\
 (\rho_{b,n+1;a,n})^* &= \rho_{a,n;b,n+1} = i(P_n \rho_{aa} - P_{n+1} \rho_{bb}) S_{n+1} C_{n+1} \\
 (\rho_{b,n+1;b,n})^* &= \rho_{b,n;b,n+1} = i P_n \rho_{ba} S_{n+1} C_n \\
 (\rho_{a,n;b,n})^* &= \rho_{b,n;a,n} = P_n \rho_{ba} C_n C_{n+1} \\
 (\rho_{a,n+1;a,n})^* &= \rho_{a,n;a,n+1} = -i P_{n+1} \rho_{ba} S_{n+1} C_{n+2}.
 \end{aligned} \tag{2.8}$$

This is a local operation which means it only operates on the field state. Note that no local operations can give an entangled outcome from a separable state. Due to this fact, we can use the Peres' criterion to check the entanglement of $(\hat{\rho}_{af})_n$ and we have if $(\hat{\rho}_{af})_n$ is entangled, the original state (2.5) is also entangled. Furthermore, we note that we cannot specify n if we actually do the projection. We have to sum over all outcomes weighted by the probability to get this outcome for all n 's. Therefore, it is better to use the following quantity to estimate the entanglement:

$$E(\rho_{af}(t)) = -2 \sum_{n=0,2,4,\dots}^{\infty} p_n \lambda_n^-, \tag{2.9}$$

where λ_n^- is the negative eigenvalue (if no negative eigenvalue, then $\lambda_n^- = 0$) of the partial transposed matrix of ρ_{af}^n . p_n is the probability of obtaining ρ_{af}^n when we do the projection. This is actually the weighted average of entanglement of ρ_{af}^n over all

possible values of n . If $E(\rho_{af}(t))$ is positive then the state $\rho_{af}(t)$ is entangled.

3. Temperature difference as an important role in entanglement creation

Let's now estimate the entanglement of state (2.5). We first consider the case when there is no atomic coherence, that is $\rho_{ab} = \rho_{ba} = 0$. For this case, the initial separable state is

$$\hat{\rho}_{af}(0) = \sum_{n=0}^{\infty} P_n |n\rangle\langle n| \otimes (\rho_{aa}|a\rangle\langle a| + \rho_{bb}|b\rangle\langle b|). \quad (2.10)$$

With the absence of the atomic coherence, we can define the temperature of the atom as $e^{\hbar\omega_{ab}/k_B T_a} = \rho_{bb}/\rho_{aa}$, where T_a is the temperature of the atom. When the atom and the field are initially in thermal equilibrium, that is $T_a = T_f$, we have [52]

$$\frac{\rho_{aa}^0}{\rho_{bb}^0} = \frac{P_{n+1}}{P_n}. \quad (2.11)$$

By putting (2.11) into equation (2.5) and (2.6) and set the atomic coherence to be zero, we can verify

$$\hat{\rho}_{af}(t) = \hat{\rho}_{af}(0). \quad (2.12)$$

This means the state will be separable for all the time, thus, no entanglement will be produced. Generally, $\hat{\rho}_{af}(t) \neq \hat{\rho}_{af}(0)$, we need to use the Peres' criterion to estimate the entanglement. We follow the procedure we discussed in section (2). Actually we just need to set the atomic coherence related matrix elements in eqn. (2.8) all to be zero. We then have

$$(\hat{\rho}_{af})_n = \begin{pmatrix} \rho_{b,n;b,n} & 0 & 0 & 0 \\ 0 & \rho_{b,n+1;b,n+1} & \rho_{b,n+1;a,n} & 0 \\ 0 & \rho_{a,n;b,n+1} & \rho_{a,n;a,n} & 0 \\ 0 & 0 & 0 & \rho_{a,n+1;a,n+1} \end{pmatrix}. \quad (2.13)$$

Now, if we partially transpose $(\hat{\rho}_{af})_n$ and try to calculate its eigenvalues, we can find the only possible negative eigenvalue will be

$$\lambda_n = \frac{\eta_n - \sqrt{\eta_n^2 - 4\xi_n}}{2}, \quad (2.14)$$

where

$$\begin{aligned}\eta_n &= \rho_{b,n;b,n} + \rho_{a,n+1;a,n+1} \\ \xi_n &= \rho_{b,n;b,n}\rho_{a,n+1;a,n+1} - |\rho_{a,n;b,n+1}|^2.\end{aligned}\tag{2.15}$$

Whenever ξ_n is negative, λ_n will also be negative, thus $(\hat{\rho}_{af})_n$ as well as $\hat{\rho}_{af}(t)$ will be entangled. The inequality $\xi_n < 0$ can be rewritten as

$$a_n x^2 + b_n x + c_n > 0,\tag{2.16}$$

where

$$\begin{aligned}a_n &= S_{n+1}^2 C_{n+1}^2 - C_n^2 S_{n+2}^2, \\ b_n &= -(C_n^2 C_{n+2}^2 + S_n^2 S_{n+2}^2 + 2S_{n+1}^2 C_{n+1}^2), \\ c_n &= (S_{n+1}^2 C_{n+1}^2 - S_n^2 C_{n+2}^2), \\ x &= \frac{\langle n \rangle}{1 + \langle n \rangle} \frac{\rho_{bb}^0}{\rho_{aa}^0} = e^{-(\gamma_a - \gamma_f)},\end{aligned}\tag{2.17}$$

and $\gamma = -\hbar\nu/k_B T$ is the dimensionless temperature we define for convenience. Here we have explicitly put in the expressions for those matrix elements which have been shown in eqn. (2.8).

Just for an examination, we again consider the case when the system is in thermal equilibrium. In this case, $\gamma_a = \gamma_f (T_a = T_f)$ and we have $x = 1$. Put this back into (2.16), the left hand side becomes $a_n + b_n + c_n$ which can be verified to be -1, the inequality never holds no matter what values of n and time t we choose. This means no entanglement can be detected all the time. This is consistent with the result we obtained by direct calculation.

The case when the atom is initially in its excited state $|a\rangle$ corresponds to $\gamma_a = +\infty (T_a = 0^-)$. By noticing physically γ_f can only be in $(-\infty, 0]$ (that is $T_f \in$

$[0, +\infty)$), we always have the temperature difference $\gamma_a - \gamma_f = +\infty$ and thus $x = 0$. Inequality (2.16) then becomes $c_n = S_{n+1}^2 C_{n+1}^2 - S_n^2 C_{n+2}^2 > 0$. This case has been discussed by S. Bose et. al. [47] in a great detail. We notice that no matter what temperature the thermal field has, due to the oscillation of c_n and the change of period of c_n with respect to n , for an arbitrary time t ($t \neq 0$), we can always find an n which makes the inequality (2.16) holds. This means there is entanglement at all instants of time t except for $t = 0$ for an arbitrarily high-temperature thermal field.

Another interesting case would be when the atom is initially in its ground state (that is, $\gamma_a = -\infty$ ($T_a = 0^+$)) and the field has an infinite high temperature (that is, $\gamma_f = 0$ ($T_f = +\infty$)). In this case, the temperature difference between the atom and the field will be $\gamma_a - \gamma_f = -\infty$ and $x = +\infty$, the inequality becomes $a_n = S_{n+1}^2 C_{n+1}^2 - C_n^2 S_{n+2}^2 > 0$. The same kind of argument for the previous case can then be applied to conclude that entanglement exists for all instants of time t except for $t = 0$.

So far we have discussed the entanglement of the atom-field system under some extreme conditions. From these discussions, we may guess that the temperature difference between the atom and the field may play an important role to determine the creation of entanglement for our atom-field system. Let's now discuss the general case to see this issue more clearly. As a matter of fact, one can easily verify that the discriminant of inequality (2.16) $\Delta_n = b_n^2 - 4a_n c_n$ is always positive for any n and time t . We show solutions of (2.16) in table (I). In table (I), all right hand side of inequalities in the third row must be positive, otherwise $\gamma_a - \gamma_f = 0$ thus $x = 1$ would be a suitable solution of inequality (2.16) which will conflict with our previous results. From table (I), we can see for a given time t we can always find the lower critical points for $\gamma_a - \gamma_f$ and $\gamma_f - \gamma_a$, when the temperature difference, either $\gamma_a - \gamma_f$ or $\gamma_f - \gamma_a$, is bigger than its corresponding critical point, inequality (2.16) will hold

Table I. Solutions of inequality (2.16)

$a_n > 0$	$a_n < 0$	$a_n = 0$
$x < \frac{-b_n - \sqrt{\Delta_n}}{2a_n}$ or $x > \frac{-b_n + \sqrt{\Delta_n}}{2a_n}$	$x < \frac{-b_n - \sqrt{\Delta_n}}{2a_n}$	$x > -\frac{c_n}{b_n}$
$\gamma_a - \gamma_f > -\ln\left(\frac{-b_n - \sqrt{\Delta_n}}{2a_n}\right)$ or $\gamma_f - \gamma_a > \ln\left(\frac{-b_n + \sqrt{\Delta_n}}{2a_n}\right)$	$\gamma_a - \gamma_f > -\ln\left(\frac{-b_n - \sqrt{\Delta_n}}{2a_n}\right)$	$\gamma_f - \gamma_a > \ln\left(-\frac{c_n}{b_n}\right)$

for a specific value of n , the system is thus in an entangled state. We can then argue that whether or not we have entanglement will depend on the temperature difference between the atom and the field rather than the absolute values of the temperatures. It is hard to calculate those critical points analytically since we must compare the results for all values of n . Nevertheless, we can still do numerical calculations to show this behavior.

Fig. 4 shows our numerical results of $E(\rho_{af}(t))$ for different temperature of atom, where we have fixed the dimensionless temperature of the field as $\gamma_f = -0.01$ which corresponds to the average photon number of the field $\langle n \rangle = 100$. Note here, we have used the weighted entanglement measure we defined in (2.9) to estimate the entanglement. This figure clearly shows that a sufficiently large temperature difference is the main factor to determine whether or not entanglement can be created in an atom-field interaction system.

4. Control of entanglement creation

We know no entanglement can be produced if the atom and the field are in thermal equilibrium. A question is “is there anyway we can make the system deviate from the thermal equilibrium and create entanglement?” Actually, this can be easily done.

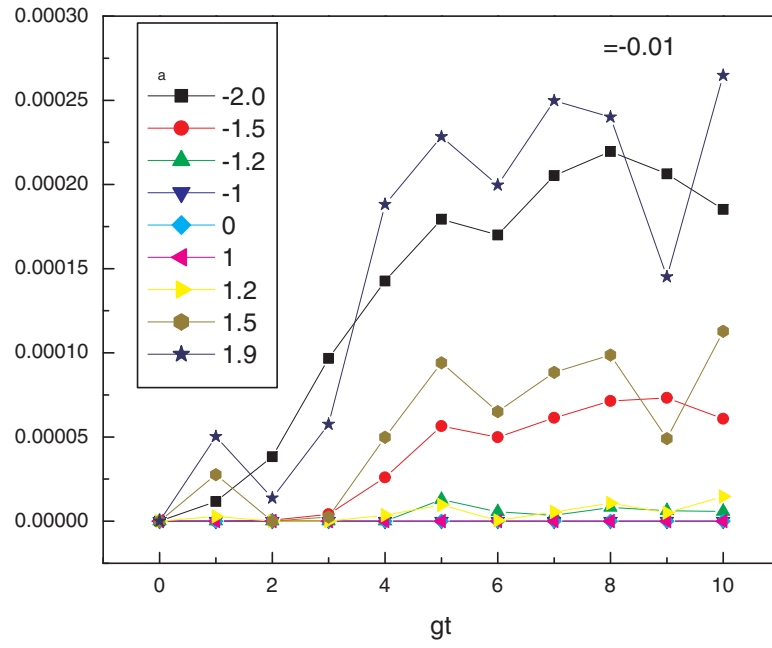


Fig. 4. Entanglement dependance on time for different temperature of atoms.
 $\gamma_f = -0.01$ and $\langle n \rangle = 100$ for the thermal field

We can just simply let the atom pass through a strong classical field, we know the population distribution of the atom can be dramatically changed by the interaction with the classical field. Although this will be accompanied by the production of atomic coherence, we can still only concentrate on the population distribution and define the phenomenal dimensionless temperature as before, $\rho_{bb}/\rho_{aa} = e^{-\gamma_a}$, where γ_a is the dimensionless temperature. By choosing different interaction time, we can get different γ_a 's. The atom then can interact with the quantized field and produce entanglement. Fig (5) shows the numerical result of the entanglement creation of the quantized system with respect to different passage time of the classical system. We can see that entanglement oscillates with respect to the passage time, when $g\tau = \pi/2$ (τ is the passage time, this corresponds to a π pulse), the population is maximally inverted and entanglement reaches a maximum. By using this strategy we may control the creation of entanglement of the system.

So far, we have discussed the creation of entanglement between a two-level atom and a thermal field in this section. We show that the temperature difference rather than the temperatures themselves of the atom-field system act an important role in this creation. We also show that the entanglement can be controlled by interacting the atom with a strong classical field. This will give us flexibility for different usage of this system.

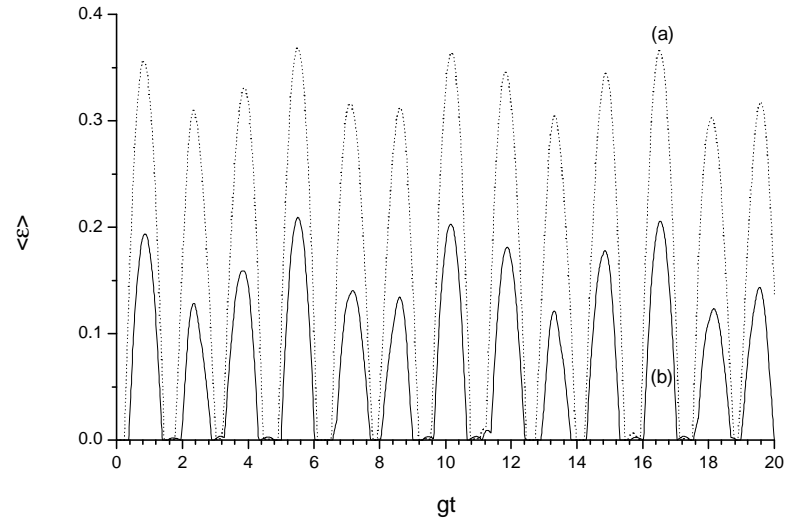


Fig. 5. Entanglement dependance on the passage time of the atom through the classical field, $\Omega\tau = \pi/2.0$, (a) $\langle n \rangle = 0.3$; (b) $\langle n \rangle = 0.5$

B. Coherence induced entanglement*

In this section, we discuss a very important system where atomic coherence plays a crucial role in creating entanglement between two modes of the electromagnetic field inside a doubly resonant cavity at temperature T . The two modes of the field are coupled to two transitions of a three-level atom in “V” configuration. The two important concepts, entanglement and atomic coherence, are shown to be closely related.

In earlier studies on the interaction of thermal fields with the atomic systems, it has been shown that atom-field [47] and atom-atom [53] entanglement can be generated in such systems. In these studies, at least, one subsystem is initially in a pure state. The entanglement appears only when the atom and the field are not in thermal equilibrium. Here we show that atomic coherence is the unique resource of creating entanglement between two cavity modes in thermal state even at arbitrarily high temperature.

1. System description and the Hamiltonian

The model under consideration is shown in Fig. 6. We consider the interaction of an atom in the V configuration with the fields inside a cavity at temperature T . Here we assume that the transitions between the upper levels $|a\rangle$ and $|b\rangle$ to the ground state $|c\rangle$ are dipole allowed and these transitions are coupled resonantly with the

*Reprinted with permission from Fuli Li, Han Xiong and M. Suhail Zubairy, Phys. Rev. A 72, 010303, (2005). Copyright (2005) by the American Physical Society.

Readers may view, browse, and/or download material for temporary copying purposes only, provided these uses are for noncommercial personal purposes. Except as provided by law, this material may not be further reproduced, distributed, transmitted, modified, adapted, performed, displayed, published, or sold in whole or part, without prior written permission from the publisher.

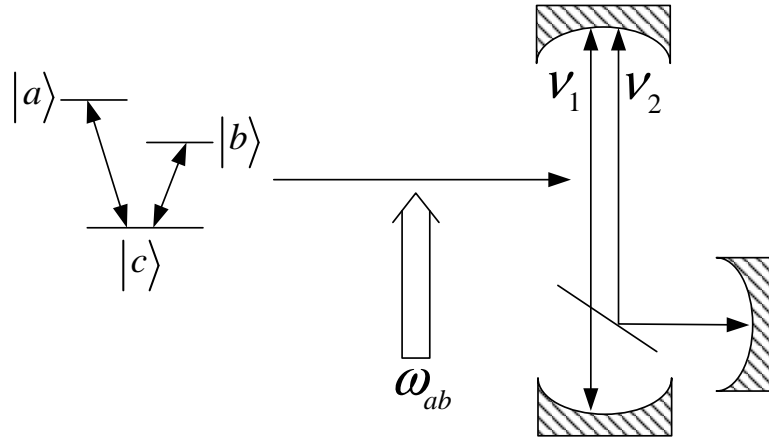


Fig. 6. A three-level atom in “V” configuration with initial populations $\rho_{aa}, \rho_{bb}, \rho_{cc}$ is prepared in a superposition of upper level $|a\rangle$ and $|b\rangle$ by a resonant classical field. The atom then passes through a doubly resonant cavity which is resonant with $|a\rangle - |c\rangle$ and $|b\rangle - |c\rangle$ transitions. The fields inside the cavity are initially diagonal, such as a thermal state.

modes inside the cavity. The transition between the upper levels $|a\rangle$ and $|b\rangle$ is dipole forbidden, while the coherence between level $|a\rangle$ and level $|b\rangle$ could be created by applying a classical magnetic field between these two levels. The interaction picture Hamiltonian of the system is given by

$$\hat{H} = \hbar g_1(|a\rangle\langle c|\hat{a}_1 + |c\rangle\langle a|\hat{a}_1^\dagger) + \hbar g_2(|b\rangle\langle c|\hat{a}_2 + |c\rangle\langle b|\hat{a}_2^\dagger), \quad (2.18)$$

where $\hat{a}_1(\hat{a}_1^\dagger)$ and $\hat{a}_2(\hat{a}_2^\dagger)$ are the annihilation (creation) operators for the two cavity modes and $g_{1,2}$ are coupling constants of the atom with the fields.

2. Entanglement generation via atomic coherence

We consider the initial states of the cavity fields to be diagonal in the Fock-state representation and the atom to be prepared in a coherent superposition of the upper levels by a classical field of frequency ω_{ab} as shown in Fig. 6. The initial state of the atom-field system is written as

$$\begin{aligned} \hat{\rho}_{af}(0) = & \sum_{n_1=0}^{\infty} P_{n_1}|n_1\rangle\langle n_1| \otimes \sum_{n_2=0}^{\infty} P_{n_2}|n_2\rangle\langle n_2| \\ & \otimes (\rho_{aa}|a\rangle\langle a| + \rho_{bb}|b\rangle\langle b| + \rho_{cc}|c\rangle\langle c| + \rho_{ab}|a\rangle\langle b| + \rho_{ba}|b\rangle\langle a|), \end{aligned} \quad (2.19)$$

where $P_{n_{1,2}}$ are the probabilities for having photon number states $|n_{1,2}\rangle$. An example of fields with vanishing off-diagonal matrix elements in the Fock-state representation is a thermal state, which has $P_{n_{1,2}} = \frac{\langle n_{1,2} \rangle^{n_{1,2}}}{(1+\langle n_{1,2} \rangle)^{n_{1,2}+1}}$. Here $\langle n_{1,2} \rangle = (e^{\hbar\nu_{1,2}\beta} - 1)^{-1}$ are the mean photon number of the fields at temperature T with $\nu_{1,2}$ being the field frequencies, and $\beta^{-1} = k_B T$ with k_B being the Boltzmann constant.

The density matrix operator at time t is given by $\hat{\rho}_{af}(t) = \hat{U}(t)\hat{\rho}_{af}(0)\hat{U}^\dagger(t)$ where $\hat{U}(t) = \exp(-i\hat{H}t/\hbar)$ is the time evolution operator. It follows, on taking a trace over

the atomic variables, that the reduced density matrix operator for the fields is given by

$$\begin{aligned}
\hat{\rho}_f(t) = & \sum_{n_1=0}^{\infty} \sum_{n_2=0}^{\infty} \rho_{n_1, n_2; n_1, n_2} |n_1, n_2\rangle \langle n_1, n_2| \\
& + \rho_{ab} \sum_{n_1=0}^{\infty} \sum_{n_2=0}^{\infty} \rho_{n_1+1, n_2; n_1, n_2+1} |n_1+1, n_2\rangle \langle n_1, n_2+1| \\
& + \rho_{ba} \sum_{n_1=0}^{\infty} \sum_{n_2=0}^{\infty} \rho_{n_1, n_2+1; n_1+1, n_2} |n_1, n_2+1\rangle \langle n_1+1, n_2|,
\end{aligned} \tag{2.20}$$

where the matrix elements are given by

$$\begin{aligned}
\rho_{n_1, n_2; n_1, n_2} &= P_{n_1} P_{n_2} \\
&\{ \rho_{aa} [1 - g_1^2 (n_1 + 1) A_{n_1+1, n_2} (1 - C_{n_1+1, n_2})]^2 \\
&+ \rho_{bb} [1 - g_2^2 (n_2 + 1) A_{n_1, n_2+1} (1 - C_{n_1, n_2+1})]^2 \} \\
&+ g_1^2 g_2^2 \{ \rho_{aa} P_{n_1-1} P_{n_2+1} n_1 (n_2 + 1) \\
&\times A_{n_1, n_2+1}^2 (1 - C_{n_1, n_2+1})^2 \\
&+ \rho_{bb} P_{n_1+1} P_{n_2-1} n_2 (n_1 + 1) A_{n_1+1, n_2}^2 (1 - C_{n_1+1, n_2})^2 \} \\
&+ \{ \rho_{aa} P_{n_1-1} P_{n_2} g_1^2 n_1 + \rho_{bb} P_{n_1} P_{n_2-1} g_2^2 n_2 \} A_{n_1, n_2} S_{n_1, n_2}^2 \\
&+ \rho_{cc} \{ P_{n_1} P_{n_2} C_{n_1, n_2}^2 \\
&+ P_{n_1+1} P_{n_2} g_1^2 (n_1 + 1) A_{n_1+1, n_2} S_{n_1+1, n_2}^2 \\
&+ P_{n_1} P_{n_2+1} g_2^2 (n_2 + 1) A_{n_1, n_2+2} S_{n_1, n_2+1}^2 \}, \tag{2.21}
\end{aligned}$$

$$\begin{aligned}
\rho_{n_1+1, n_2; n_1, n_2+1} &= -g_1 g_2 \sqrt{(n_1 + 1)(n_2 + 1)} \\
&\times \{ A_{n_1+1, n_2+1} (1 - C_{n_1+1, n_2+1}) \\
&\times (P_{n_1+1} P_{n_2} [1 - g_1^2 (n_1 + 2) A_{n_1+2, n_2} (1 - C_{n_1+2, n_2})] \\
&+ P_{n_1} P_{n_2+1} [1 - g_2^2 (n_2 + 2) A_{n_1, n_2+2} (1 - C_{n_1, n_2+2})]) \\
&- P_{n_1} P_{n_2} \sqrt{A_{n_1+1, n_2} A_{n_1, n_2+1}} S_{n_1+1, n_2} S_{n_1, n_2+1} \}, \tag{2.22}
\end{aligned}$$

$$\rho_{n_1, n_2+1; n_1+1, n_2} = (\rho_{n_1+1, n_2; n_1, n_2+1})^*, \tag{2.23}$$

with $A_{n_1, n_2} = (g_1^2 n_1 + g_2^2 n_2)^{-1}$, $S_{n_1, n_2} = \sin(\sqrt{g_1^2 n_1 + g_2^2 n_2} t)$ and $C_{n_1, n_2} = \cos(\sqrt{g_1^2 n_1 + g_2^2 n_2} t)$.

We first discuss the case where initially there is no atomic coherence, i.e., $\rho_{ab} = \rho_{ba} = 0$. It is clear from Eq. (2.20) that, under this condition, the fields are definitely

in a separable state:

$$\hat{\rho}_f(t) = \sum_{n_1=0}^{\infty} \sum_{n_2=0}^{\infty} \rho_{n_1, n_2; n_1, n_2} |n_1, n_2\rangle \langle n_1, n_2|. \quad (2.24)$$

In this case, the fields may still have classical statistical correlation if $\rho_{n_1, n_2; n_1, n_2}$ can not be decomposed into a direct product of the form $\rho_{n_1, n_1} \otimes \rho_{n_2, n_2}$. As a special case, we consider the situation where the atom and the fields are initially in thermal equilibrium. In this case, the level populations of the atom are determined by the relations $\frac{\rho_{aa}}{\rho_{cc}} = \frac{\langle n_1 \rangle}{\langle n_1 \rangle + 1}$, $\frac{\rho_{bb}}{\rho_{cc}} = \frac{\langle n_2 \rangle}{\langle n_2 \rangle + 1}$. It follows, on substituting these relations in Eq. (2.21), that state (2.24) becomes

$$\rho_f = \sum_{n_1=0}^{\infty} P_{n_1} |n_1\rangle \langle n_1| \otimes \sum_{n_2=0}^{\infty} P_{n_2} |n_2\rangle \langle n_2|, \quad (2.25)$$

i.e., we have neither entanglement nor classical correlation between the fields as the two fields are completely separable.

So how do we entangle the thermal fields? We show that this can be accomplished via atomic coherence.

In Eqs. (2.21), the term proportional to the population of the level $|c\rangle$ results from one-photon absorption processes. The photon absorption processes lead to the classical correlation between the fields and have no contribution to the entanglement. Therefore, in order to create strong entanglement, the population of the level $|c\rangle$ should be reduced. In Eq. (2.22), the terms related to $P_{n_1+1}P_{n_2}$ and $P_{n_1}P_{n_2+1}$ involve the processes in which one mode photon is emitted and another mode photon is absorbed, and the term proportional to $P_{n_1}P_{n_2}$ comes from the photon emission processes of the upper levels. If the atomic coherence exists, these terms contribute to the off-diagonal matrix elements. Without the off-diagonal correlation contribution given in Eqs. (2.22) and (2.23), the fields have no entanglement. However, the

existence of the off-diagonal correlation can not guarantee entanglement. Thus, we need to find a condition for the existence of entanglement between the fields in the state (2.20).

State (2.20) is defined in an infinite dimensional Hilbert space. In general, it is very difficult to measure the entanglement in such systems [47] [53]. However, we can apply the same trick as we have used in section (A). We recall that entanglement can not be generated through local transformations. To estimate the entanglement of (2.20), we consider the local projection operators $\hat{A}_{n_1} = |n_1\rangle\langle n_1| + |n_1 + 1\rangle\langle n_1 + 1|$ and $\hat{B}_{n_2} = |n_2\rangle\langle n_2| + |n_2 + 1\rangle\langle n_2 + 1|$ with $n_{1,2} = 0, 2, 4, \dots$. If the fields are in a separable state $\sum_i p_i \rho_i^{(1)} \otimes \rho_i^{(2)}$, the projected state $\hat{A}_{n_1} \hat{B}_{n_2} \sum_i p_i \rho_i^{(1)} \otimes \rho_i^{(2)} \hat{B}_{n_2}^\dagger \hat{A}_{n_1}^\dagger$ is still separable. Then we can claim the existence of entanglement in (2.20) if the entanglement exists in the projected state.

The projection of (2.20) on the subspace spanned by basis vectors $(|n_1\rangle, |n_1 + 1\rangle) \otimes (|n_2\rangle, |n_2 + 1\rangle)$ with fixed photon numbers $n_{1,2}(= 0, 2, 4, \dots)$ leads to the state

$$[\hat{\rho}_f(t)]_{n_1, n_2} = \hat{A}_{n_1} \hat{B}_{n_2} \hat{\rho}_f(t) \hat{B}_{n_2}^\dagger \hat{A}_{n_1}^\dagger. \quad (2.26)$$

In the subspace under consideration, the projected density matrix operator (2.26) becomes a 4×4 hermitian matrix. Now we can apply the Peres-Horodecki sufficiency condition [49, 50] for the inseparability of density matrices of a two-party quantum system.

The partial transposition of the density matrix (2.26) has a negative eigenvalue if the condition

$$|\rho_{ab}|^2 > R_{n_1, n_2} = \frac{\rho_{n_1, n_2; n_1, n_2} \rho_{n_1+1, n_2+1; n_1+1, n_2+1}}{|\rho_{n_1+1, n_2; n_1, n_2+1}|^2} \quad (2.27)$$

is satisfied. According to the Peres-Horodecki condition, we can claim that state (2.20) is an entangled state if the condition (2.27) is satisfied. This kind of methodology to

detect the entanglement of an infinite dimensional mixed state for a bipartite system was first discussed and used in reference [47].

Experimentally, the verification of inequality (2.27) requires the full knowledge of the state. Several schemes have been proposed to reconstruct a two-mode state in a high-Q cavity recently [54]. For example, one can look at the spontaneous emission spectrum in a driven four-level atomic system passing through the cavity to recover the Wigner function of the two-mode field [55]. Once the Wigner function is known, the right hand side of (2.27) can be calculated in a straightforward manner.

It follows from Eqs. (2.21) and (2.22) that $R_{0,0} = 0$ when $\langle n_1 \rangle$ and $\langle n_2 \rangle$ approach zero. Thus, for this case, arbitrarily small but nonzero atomic coherence can induce entanglement between the two modes. For a general case, R_{n_1, n_2} is always larger than zero. Therefore there is the minimum atomic coherence beyond which the entanglement can appear. The right side of (2.27) depends on the level populations which satisfy the physical restriction with respect to the atomic coherence: $\rho_{aa}\rho_{bb} \geq |\rho_{ab}|^2$. In order to conveniently control the populations and atomic coherence at the same time, we consider the atom whose level populations initially are $\rho_{ii}(0)$ ($i = a, b, c$) and off diagonal matrix elements $\rho_{ij} = 0$ for $i \neq j$. A coherence between the excited states a and b is created when the atom interacts resonantly with a classical magnetic field (since this transition is dipole forbidden) of frequency ω_{ab} for a time τ . After the interaction with the classical field, the populations and the atomic coherence are given by [56]

$$\begin{aligned}\rho_{aa} &= \rho_{aa}(0) \cos^2(\Omega\tau) + \rho_{bb}(0) \sin^2(\Omega\tau), \\ \rho_{bb} &= \rho_{aa}(0) \sin^2(\Omega\tau) + \rho_{bb}(0) \cos^2(\Omega\tau), \\ \rho_{ab} &= (\rho_{ba})^* = ie^{i\theta}(\rho_{aa}(0) - \rho_{bb}(0)) \sin(\Omega\tau) \cos(\Omega\tau),\end{aligned}\tag{2.28}$$

where Ω is the Rabi frequency and θ is the phase of the driving field. All the other density matrix elements remain unchanged. In this way, we can unitarily and continuously control the level populations and atomic coherence by use of the single parameter $\Omega\tau$. After passing through the classical field, the atom acquires a coherence. When this atom passes through the cavity with two thermal fields, the state of the fields is described by the density matrix (2.20). The entanglement of the resulting state of the field is determined by the condition (2.27).

In Fig. 7, the right side of (2.27) with $n_1 = n_2 = 0$ and the squared modulus of the atomic coherence (2.28) are shown as a function of $\Omega\tau$ when the atom and the fields are initially in thermal equilibrium. In the present calculation, we take $g_1 = g_2 = g$. We also find that, as a function of n_1 and n_2 , the right side of the inequality (2.27) takes the minimal value with $n_1 = n_2 = 0$. From Fig. 7, it can be noticed that the entanglement condition (2.27) can be satisfied if the difference between the mean thermal photon numbers of the two fields is sufficiently large. This situation may not easily be realizable because it requires a large frequency difference between the two upper levels.

Eq.(2.28) shows that the atomic coherence is proportional to the population inversion of the upper levels. On the other hand, the numerator of the right side of the condition (2.27) decreases if the level populations ρ_{aa}, ρ_{bb} or ρ_{cc} are small. Therefore, the best initial condition of the atom for satisfying the condition (2.27) is that the atom is in one of the upper levels. For this case, Fig. 8 shows that the entanglement condition (2.27) can be satisfied even if the temperature becomes arbitrarily high.

As discussed earlier, the Hilbert space for the complete system is infinite dimensional, i.e., the dimension of the density matrix (2.20) is infinite. We can therefore obtain an infinite number of the projected 4×4 hermitian matrices (2.26) with dif-

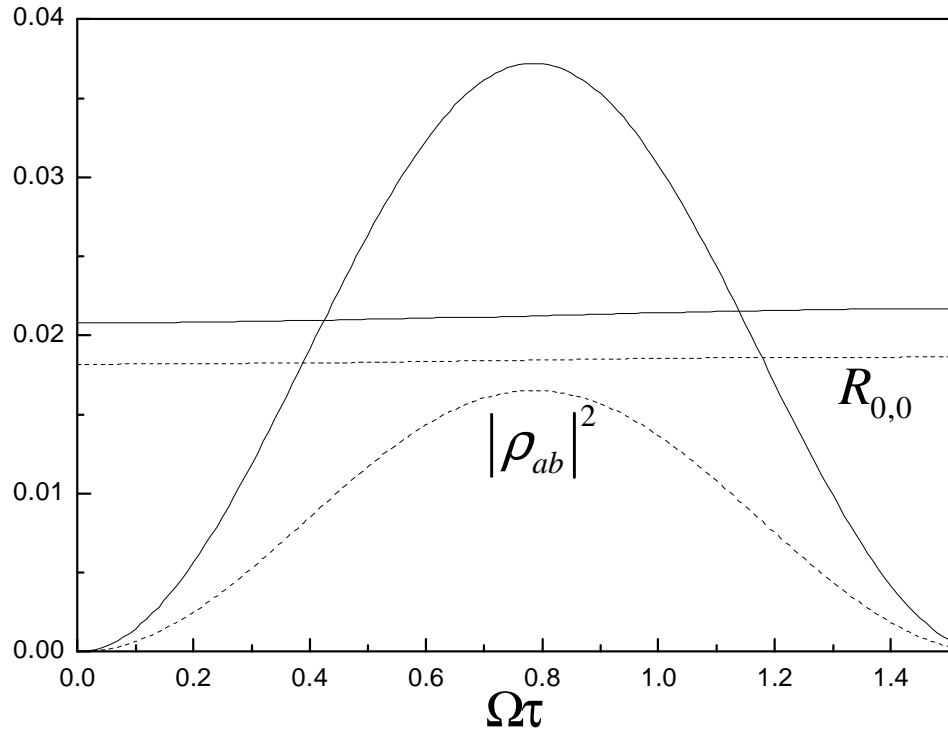


Fig. 7. The solid lines are for the case with $\langle n_1 \rangle = 0.1$ and $\langle n_2 \rangle = 5.0$. The dashed lines are for the case with $\langle n_1 \rangle = 0.1$ and $\langle n_2 \rangle = 1.0$. $g\tau=11.0$.

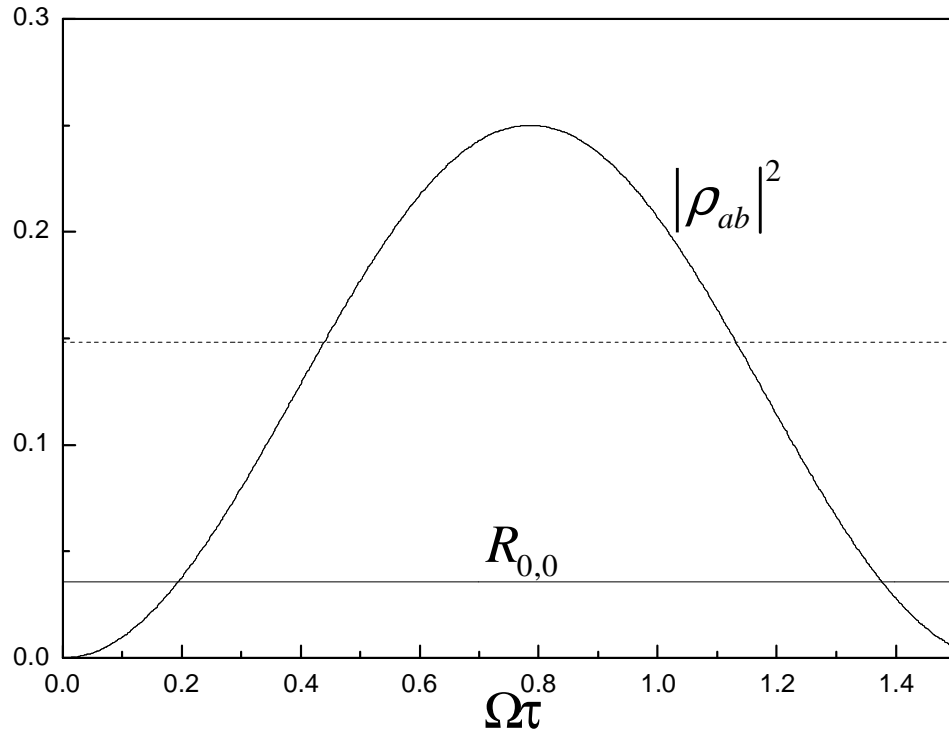


Fig. 8. The solid lines are for the case with $\langle n_1 \rangle = \langle n_2 \rangle = 1.0$. The dashed line is for the case with $T \rightarrow \infty$, $gt=5.0$ and $\rho_{aa} = 1$.

ferent photon numbers n_1 and n_2 by projecting the density matrix (2.20) into the subspaces. We can then use the quantity [57]

$$\langle \mathcal{E} \rangle = -2 \sum_{n_1, n_2=0,2,4,\dots}^{\infty} p_{n_1, n_2} \lambda_{n_1, n_2} \quad (2.29)$$

to measure the entanglement of (2.20), where λ_{n_1, n_2} is the negative eigenvalue of the partial transposed density matrix of (2.26) and $p_{n_1, n_2} = \rho_{n_1, n_2; n_1, n_2} + \rho_{n_1+1, n_2; n_1, n_2} + \rho_{n_1, n_2+1; n_1, n_2} + \rho_{n_1+1, n_2+1; n_1+1, n_2+1}$ is the probability of taking the 4×4 matrix (2.26) out of the matrix (2.20). If $\langle \mathcal{E} \rangle = 0$, it does not mean non entanglement. If $\langle \mathcal{E} \rangle \neq 0$, however, we can ensure that the infinite dimensional density matrix (2.20) must be an entangled state. In Fig. 9, the time evolution of the entanglement (2.29) is shown when the atom and the fields are initially in thermal equilibrium. It is seen that for this case the weak entanglement is detected at several time points. As pointed out earlier, the atomic coherence will become stronger when the atom is initially in one of the upper level. Therefore, we may expect that in this case the stronger entanglement will be detected. Fig. 10 shows the time evolution of the entanglement (2.29) when the atom is initially in the level $|a\rangle$.

In conclusion we have shown that, no matter how high the temperature is, and the atom and the fields are initially in either thermal nonequilibrium or equilibrium, two thermal field modes in a cavity can be entangled by a single three-level atom of the V-configuration when the coherence between two upper levels is beyond a critical value. The present result reveals a relation between entanglement and atomic coherence.

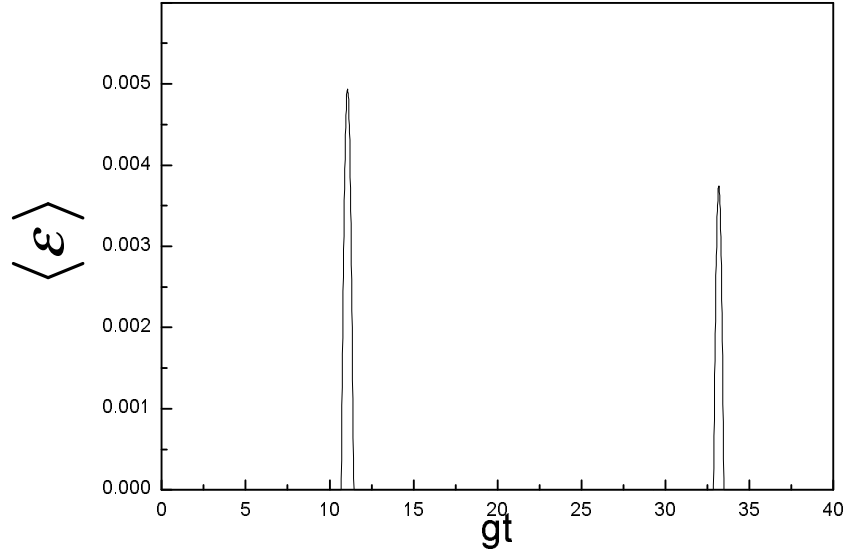


Fig. 9. The time evolution of the entanglement measurement with $\langle n_1 \rangle = 0.1$, $\langle n_2 \rangle = 5.0$, and $\Omega\tau = \pi/4$.

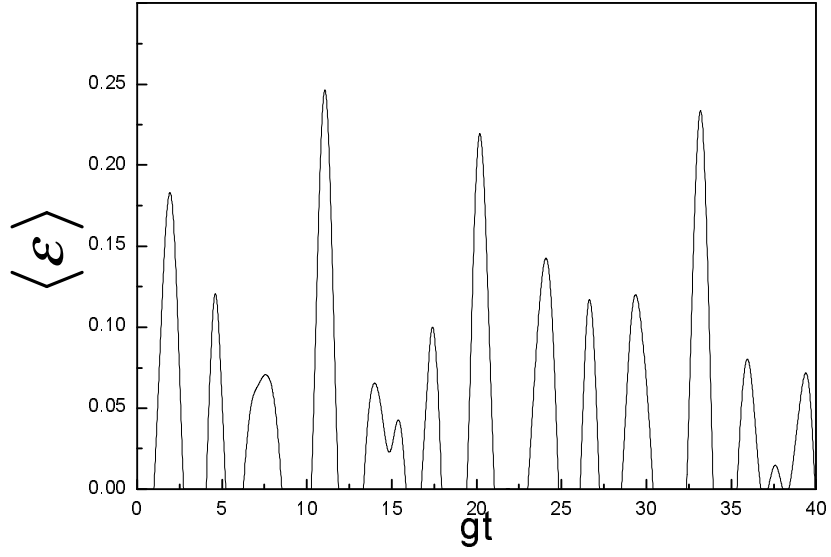


Fig. 10. The time evolution of the entanglement measurement with $\langle n_1 \rangle = 1.0$, $\langle n_2 \rangle = 1.0$, and $\Omega\tau = \pi/4$ and $\rho_{aa} = 1$.

CHAPTER III

CORRELATED SPONTANEOUS EMISSION LASER AS ENTANGLEMENT SOURCES

In the previous section, we have seen that atomic coherence is necessary to produce entanglement between two field modes. So far our discussion is limited to the microscopic level, that is we only consider systems, which have only one atom inside the cavity. What about systems involving large number of atoms such as a laser system or a micromaser system? We ask ourselves especially with the following question: “Can we have two laser beams which are entangled to each other?”

We recall that we have encountered CEL systems in the introduction section. These systems have first been proposed to reduce the relative phase diffusion in laser systems. We now claim that they can also be used to provide macroscopically entangled laser beams. In the introduction section, we have assumed CEL systems with the injection of atomic coherence. That is, atoms are initially prepared to have atomic coherence and then injected into the cavity. Actually, atomic coherence can also be created by coherent pumping. We will see that this coherent pumping process is in fact very crucial to our entanglement generation and amplification.

A. Correlated spontaneous emission laser as an entanglement amplifier*

In order to see clearly how a CEL can lead to an entangled state, we first recall that, in a quantum beat laser [3] or a Hanle-effect laser [4], a beam of three-level atoms in the “V” configuration interacts with two modes of the field. The upper

*Reprinted with permission from Han Xiong, Marlan O. Scully and M. Suhail Zubairy Phys. Rev. Lett. Vol. 94, 023601(2005). Copyright (2005) by the American Physical Society.

levels $|a\rangle$ and $|b\rangle$ are initially prepared in a coherent superposition or are driven by a coherent field. We consider the simple case when an atom is in a superposition of upper states and there are no photons in the modes associated with the $|a\rangle \rightarrow |c\rangle$ and the $|b\rangle \rightarrow |c\rangle$ transitions, i.e., the initial state of the atom-field system is $(|a\rangle + |b\rangle)/\sqrt{2} \otimes |0, 0\rangle$. An atomic transition to the lower level $|c\rangle$ leads to the entangled state $(|1, 0\rangle + |0, 1\rangle)/\sqrt{2}$ of the field modes. It is thus clear that an amplified entangled state will be generated in a correlated emission laser. In this section we discuss different atomic configurations, such as a three-level atomic system in a cascade configuration or Raman configuration. For cascade atoms, the upper and lower levels are prepared in a coherent superposition and the photons are emitted in cascade transitions [6, 58].

1. System description and the Hamiltonian

We consider a system in which atoms interact with two modes of the field inside a doubly resonant cavity (Fig. 11a). We first consider three-level atoms in a cascade configuration (Fig. 11b). The dipole allowed transitions $|a\rangle - |b\rangle$ and $|b\rangle - |c\rangle$ are resonantly coupled with the two non-degenerate modes ν_1 and ν_2 of the cavity, while the dipole forbidden transition $|a\rangle - |c\rangle$ is induced by a semiclassical field (for example, by applying a strong magnetic field for a magnetic dipole allowed transition). We denote the Rabi frequency of this field by $\Omega e^{-i\phi}$. The interaction Hamiltonian (in the rotating-wave-approximation) for this system is given by

$$\begin{aligned}
 H_I &= \hbar g_1 (a_1 |a\rangle \langle b| + a_1^\dagger |b\rangle \langle a|) \\
 &+ \hbar g_2 (a_2 |b\rangle \langle c| + a_2^\dagger |c\rangle \langle b|) \\
 &- \frac{1}{2} \hbar \Omega (e^{-i\phi} |a\rangle \langle c| + e^{i\phi} |c\rangle \langle a|),
 \end{aligned} \tag{3.1}$$

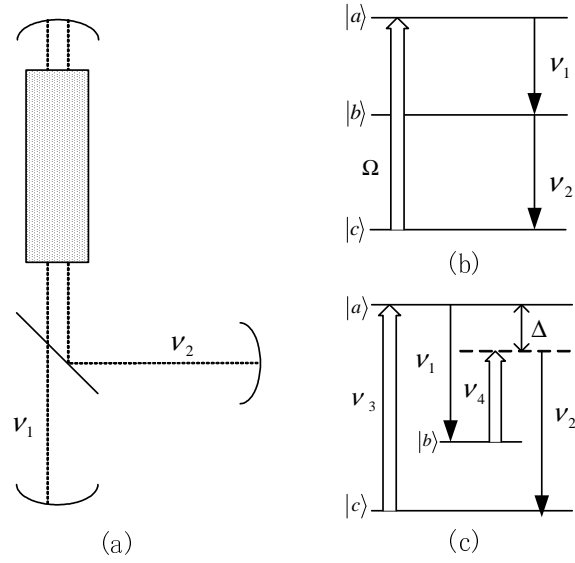


Fig. 11. (a) Schematics for the entanglement amplifier. Atomic medium is placed inside a doubly resonant cavity. (b) A three-level atomic system in a cascade configuration. The transitions between levels $|a\rangle - |b\rangle$ and levels $|b\rangle - |c\rangle$ at frequencies ν_1 and ν_2 are resonant with the cavity. The transition $|a\rangle - |c\rangle$ is dipole forbidden and can be induced by strong magnetic fields. (c) A Raman three-level atomic system where the fields of frequencies ν_3 and ν_4 are strong classical driving fields and the fields at frequencies ν_1 and ν_2 are resonant with the cavity modes.

where $a_1(a_1^\dagger)$ and $a_2(a_2^\dagger)$ are the annihilation (creation) operators of the two nondegenerate modes of the cavities and g_1 and g_2 are the associated vacuum Rabi frequencies.

A cascade system may be hard to implement experimentally as the transition between the states $|a\rangle$ and $|c\rangle$ in Fig. 11b is dipole forbidden. A more convenient system is depicted in Fig. 11c. Here atomic levels $|a\rangle$, $|b\rangle$, and $|c\rangle$ are coupled by four fields. The fields at frequencies ν_1 , ν_2 are resonant with the cavity modes and the fields of frequencies ν_3 and ν_4 with Rabi frequencies Ω_3 and Ω_4 , respectively, are classical driving fields. The classical field Ω_3 is resonant with the $|a\rangle - |c\rangle$ transition whereas the field Ω_4 is detuned from the $|a\rangle - |c\rangle$ transition by an amount Δ . Similarly the quantized field at the frequency ν_1 is assumed to be resonant with the $|a\rangle - |b\rangle$ transition and the field at frequency ν_2 is detuned from the $|a\rangle - |c\rangle$ by Δ . This system has recently been demonstrated experimentally and shows promise in applications to quantum memory in atomic systems [59, 60]. The Hamiltonian of this system in the interaction picture is:

$$\begin{aligned} H_I = & -\frac{\hbar}{2}\Omega_3 e^{-i\phi_3}|a\rangle\langle c| - \frac{\hbar}{2}\Omega_4 e^{-i\phi_4} e^{i\Delta t}|a\rangle\langle b| \\ & + \hbar g_1' a_1 |a\rangle\langle b| + \hbar g_2' a_2 e^{i\Delta t}|a\rangle\langle c| + H.c. \end{aligned} \quad (3.2)$$

When the detuning Δ is sufficiently large, the Anti-Stokes Raman transition $|b\rangle - |a\rangle - |c\rangle$ can be effectively estimated as a single transition between levels $|b\rangle$ and $|c\rangle$, and the effective Hamiltonian of the whole system can be written as

$$\begin{aligned} H_{eff} = & -\frac{\hbar}{2}\Omega_3 e^{-i\phi_3}|a\rangle\langle c| + \hbar g_1' a_1 |a\rangle\langle b| \\ & + \hbar \frac{g_2' \Omega_4}{2\Delta} e^{i\phi_4} a_2 |b\rangle\langle c| + H.c. \end{aligned} \quad (3.3)$$

Equation (3.3) is of the same form as the Hamiltonian (3.1) for the cascade system. It is therefore clear that the atomic system of the form given in Fig. 11c can be used

to implement a correlated emission laser [6, 58] and a noise-free amplifier [61]. Here we discuss its application as an entanglement amplifier.

2. Master equation

The master equation of the system in the configuration of Fig. 11b can be obtained from the Hamiltonian (3.1) by using the standard methods of laser theory. We consider only the linear theory. That is, we keep the interaction between the two quantized modes and the atoms only to its first order (the first order for probability amplitude thus the second order for the density matrix), while we treat the coherent pumping process exactly. This approximation is true if the classical pumping field is sufficiently strong and the atom-field couplings are not so strong.

The derivation of the master equation of this system is following. By tracing over the atomic states, we obtain the reduced density matrix for the field, ρ_F satisfy the following equation:

$$\begin{aligned}\dot{\rho}_F &= Tr_{atom}(\dot{\rho}) = -\frac{i}{\hbar} Tr_{atom}[H_I, \rho] \\ &= -\frac{i}{\hbar} \{ [V_{ab}\rho_{ba} + V_{ba}\rho_{ab} + V_{bc}\rho_{cb} + V_{cb}\rho_{bc}] \\ &\quad - [\rho_{ba}V_{ab} + \rho_{ab}V_{ba} + \rho_{cb}V_{bc} + \rho_{bc}V_{cb}] \},\end{aligned}\tag{3.4}$$

where

$$\begin{aligned}V_{ab} &= \hbar g_1 a_1; \quad V_{ba} = V_{ab}^\dagger = \hbar g_1 a_1^\dagger; \\ V_{bc} &= \hbar g_2 a_2; \quad V_{cb} = V_{bc}^\dagger = \hbar g_2 a_2^\dagger,\end{aligned}\tag{3.5}$$

and

$$\rho_{ij} \equiv \langle i | \rho | j \rangle, \quad i, j = a, b, c.\tag{3.6}$$

The classical driving terms didn't show up due to cancellations. The matrix elements

ρ_{ab} and ρ_{cb} can be obtained by solving the following matrix equations,

$$\dot{R} = -MR - iA, \quad (3.7)$$

where

$$R = \begin{pmatrix} \rho_{ab} \\ \rho_{cb} \end{pmatrix}, M = \begin{pmatrix} \gamma & -\frac{i}{2}\Omega e^{-i\phi} \\ -\frac{i}{2}\Omega e^{i\phi} & \gamma \end{pmatrix} \quad (3.8)$$

and

$$A = \begin{pmatrix} g_1 a_1 \rho_{bb} - g_1 \rho_{aa} a_1 - g_2 \rho_{ac} a_2^\dagger \\ g_2 a_2^\dagger \rho_{bb} - g_2 \rho_{cc} a_2^\dagger - g_1 \rho_{ca} a_1 \end{pmatrix}. \quad (3.9)$$

Note that, we have included atomic decays here. From now on, we assume all the atomic decay rates are γ for simplicity. One can also think about a micromaser system and $1/\gamma$ is the average passage time of one single atom. We now determine ρ_{aa} , ρ_{bb} , ρ_{cc} and ρ_{ac} to zeroth order of g_1 and g_2 . By setting $g_1 = g_2 = 0$ and assuming atoms are injected in the cavity in the lower level $|c\rangle$ at a rate r_a . We have $\rho_{bb}(t) = 0$ and ρ_{aa} , ρ_{cc} and ρ_{ac} satisfy the following matrix equation

$$\dot{\tilde{R}} = -\tilde{M}\tilde{R} + \tilde{B}, \quad (3.10)$$

where

$$\tilde{R} = \begin{pmatrix} \rho_{aa} \\ \rho_{ac} \\ \rho_{ca} \\ \rho_{cc} \end{pmatrix}, \tilde{M} = \begin{pmatrix} \gamma & \frac{i}{2}\Omega e^{i\phi} & -\frac{i}{2}\Omega e^{-i\phi} & 0 \\ \frac{i}{2}\Omega e^{-i\phi} & \gamma & 0 & -\frac{i}{2}\Omega e^{-i\phi} \\ -\frac{i}{2}\Omega e^{i\phi} & 0 & \gamma & \frac{i}{2}\Omega e^{i\phi} \\ 0 & -\frac{i}{2}\Omega e^{i\phi} & \frac{i}{2}\Omega e^{-i\phi} & \gamma \end{pmatrix}, \quad (3.11)$$

and

$$\tilde{B} = r_a \rho \begin{pmatrix} 0 \\ 0 \\ 0 \\ 1 \end{pmatrix}, \quad (3.12)$$

which is the atomic injection term.

equation (3.10) can be solved exactly, and we obtain

$$\tilde{R}(t) = \int_{-\infty}^t dt_0 e^{-\tilde{M}(t-t_0)} \tilde{B} = \tilde{M}^{-1} \tilde{B}. \quad (3.13)$$

The inversed matrix \tilde{M}^{-1} can be easily evaluated and we get

$$\begin{aligned} \rho_{aa} &= \frac{r_a}{2|\tilde{M}|} \gamma \Omega^2 \rho \\ \rho_{ac} &= \frac{ir_a}{2|\tilde{M}|} \gamma^2 \Omega e^{-i\phi} \rho \\ \rho_{cc} &= \frac{r_a}{|\tilde{M}|} \gamma (\gamma^2 + \Omega^2/2) \rho, \end{aligned} \quad (3.14)$$

with $|\tilde{M}| = \gamma^2(\gamma^2 + \Omega^2)$. We can now plug equation (3.14) back into equation (3.7) and use the adiabatic approximation to take the reduced density matrix $\rho(t)$ out of the integral. We then have the solution of equation (3.7) as

$$R(t) = -i \int_{-\infty}^t e^{-M(t-t_0)} dt_0 A = -i M^{-1} A, \quad (3.15)$$

where the inversed matrix

$$M^{-1} = \frac{1}{D} \begin{pmatrix} \gamma & \frac{i}{2} \Omega e^{-i\phi} \\ \frac{i}{2} \Omega e^{i\phi} & \gamma \end{pmatrix} \quad (3.16)$$

can be easily obtained. Finally we have

$$\begin{aligned}\rho_{ab} &= \frac{3ir_ag_1}{4D|\tilde{M}|}\gamma^2\Omega^2\rho_{a_1} - \frac{r_ag_2}{2D|\tilde{M}|}e^{-i\phi}(2\gamma^3\Omega + \frac{\gamma}{2}\Omega^3)\rho_{a_2}^\dagger \\ \rho_{cb} &= \frac{g_1r_a}{2D|\tilde{M}|}e^{i\phi}(\gamma^3\Omega - \frac{\gamma\Omega^3}{2})\rho_{a_1} + \frac{ig_2r_a}{D|\tilde{M}|}[\gamma^2(\gamma^2 + \frac{\Omega^2}{2}) - \frac{\gamma^2\Omega^2}{4}]\rho_{a_2}^\dagger.\end{aligned}\quad (3.17)$$

Insert the above equation into equation (3.4), the resulting equation for the reduced density operator for the cavity field modes is [62, 58].

$$\begin{aligned}\dot{\rho} &= -[\beta_{11}^*a_1a_1^\dagger\rho + \beta_{11}\rho a_1a_1^\dagger - (\beta_{11} + \beta_{11}^*)a_1^\dagger\rho a_1 \\ &+ \beta_{22}^*a_2^\dagger a_2\rho + \beta_{22}\rho a_2^\dagger a_2 - (\beta_{22} + \beta_{22}^*)a_2\rho a_2^\dagger] \\ &- [\beta_{12}^*a_1a_2\rho + \beta_{21}\rho a_1a_2 - (\beta_{12}^* + \beta_{21})a_2\rho a_1]e^{i\phi} \\ &- [\beta_{21}^*a_1^\dagger a_2^\dagger\rho + \beta_{12}\rho a_1^\dagger a_2^\dagger - (\beta_{12} + \beta_{21}^*)a_1^\dagger\rho a_2^\dagger]e^{-i\phi} \\ &- \kappa_1(a_1^\dagger a_1\rho - 2a_1\rho a_1^\dagger + \rho a_1^\dagger a_1) \\ &- \kappa_2(a_2^\dagger a_2\rho - 2a_2\rho a_2^\dagger + \rho a_2^\dagger a_2),\end{aligned}\quad (3.18)$$

where we have included the cavity damping terms in the usual way (We have assumed that the two cavity modes are coupled to two independant vacuum reservoirs here) with κ_1 and κ_2 being the the cavity decay rates of mode 1 and mode 2, respectively. The coefficients $\beta_{11}, \beta_{22}, \beta_{12}$ and β_{21} are given by

$$\beta_{11} = \frac{g_1^2 r_a}{4} \frac{3\Omega^2}{(\gamma^2 + \Omega^2)(\gamma^2 + \frac{\Omega^2}{4})}, \quad (3.19)$$

$$\beta_{22} = g_2^2 r_a \frac{1}{\gamma^2 + \Omega^2}, \quad (3.20)$$

$$\beta_{12} = g_1 g_2 r_a \frac{i\Omega}{\gamma(\gamma^2 + \Omega^2)}, \quad (3.21)$$

$$\beta_{21} = \frac{g_1 g_2 r_a}{4} \frac{i\Omega(\Omega^2 - 2\gamma^2)}{\gamma(\gamma^2 + \Omega^2)(\gamma^2 + \frac{\Omega^2}{4})}. \quad (3.22)$$

Here the terms proportional to β_{11} and β_{22} correspond to the emission from level $|a\rangle$

and absorption from level $|c\rangle$, respectively, and the terms proportional to β_{12} and β_{21} correspond to atomic coherence generated by the classical pumping field Ω .

3. Entanglement generation

We now discuss how the above system leads to entanglement amplification. In order to justify the entanglement of a state for a continuous variable system, we need an entanglement criterion. According to a criterion proposed recently [63], a state of a bipartite system is entangled if the sum of the quantum fluctuations of its two EPR-like operators \hat{u} and \hat{v} satisfy the following inequality

$$(\Delta\hat{u})^2 + (\Delta\hat{v})^2 < 2, \quad (3.23)$$

where

$$\begin{aligned} \hat{u} &= \hat{x}_1 + \hat{x}_2, \\ \hat{v} &= \hat{p}_1 - \hat{p}_2 \end{aligned} \quad (3.24)$$

and $\hat{x}_j = (a_j + a_j^\dagger)/\sqrt{2}$ and $\hat{p}_j = (a_j - a_j^\dagger)/\sqrt{2}i$ (with $j = 1, 2$) are the quadrature operators for the two subsystems 1 and 2 [63], respectively. As shown in [63], for two mode continuous variable Gaussian states, this is a necessary and sufficient criterion of entanglement. For a general mixed state, this is only a sufficient condition. Nevertheless, this sufficient criterion is good enough for our purpose here.

We first analyze the case when Ω is much greater than γ and then proceed to the general case with arbitrary Ω .

In the limit when $\Omega \gg \gamma$, we have from Eqs. (3.19)-(3.22) that

$$\beta_{11} \sim 0, \beta_{22} \sim 0, \beta_{12} \approx \beta_{21} \sim ig_1g_2r_a \frac{1}{\gamma\Omega}. \quad (3.25)$$

Under these conditions Eq. (3.18) simplifies considerably and we obtain (with $i\alpha =$

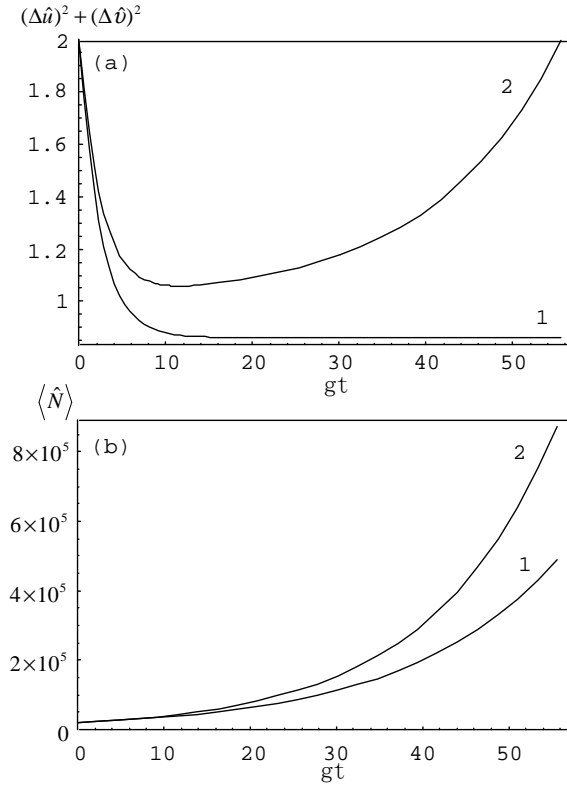


Fig. 12. (a) Time development of $(\Delta\hat{u})^2 + (\Delta\hat{v})^2$, and (b) $\langle\hat{N}\rangle$ for initial coherent states $|100, -100\rangle$ in terms of the normalized time gt . Various parameters are $r_a = 22kHz$, $g = g_1 = g_2 = 43kHz$, $\kappa = \kappa_1 = \kappa_2 = 3.85kHz$, $\gamma = 20kHz$, $\Omega = 400kHz$. In these figures, 1 and 2 represent the results for the parametric case and the general case, respectively. Parameters are chosen such that they correspond to the micromaser experiments [64].

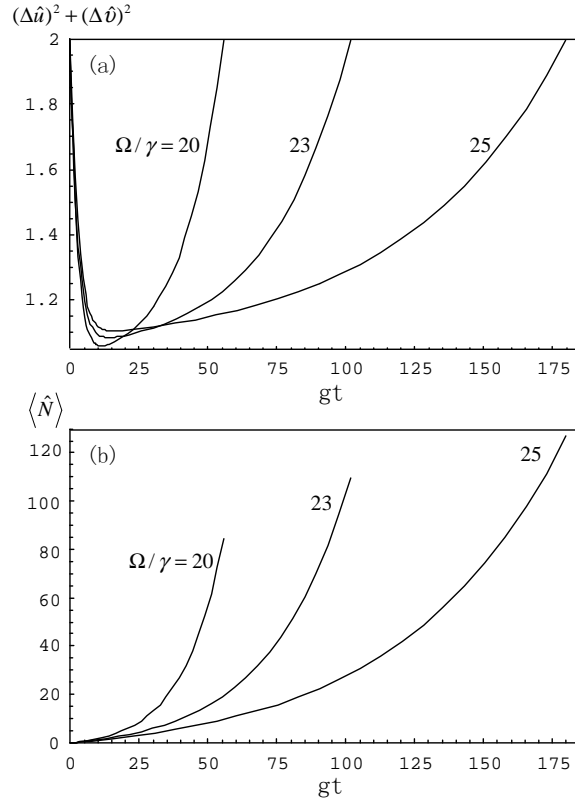


Fig. 13. (a) Time development of $(\Delta \hat{u})^2 + (\Delta \hat{v})^2$ and (b) $\langle \hat{N} \rangle$ for initial vacuum states for the two modes with $\Omega/\gamma = 20, 23, 25$. Curves in (b) are truncated when $(\Delta \hat{u})^2 + (\Delta \hat{v})^2 = 2$ and the state is not necessarily entangled. The chosen parameters are $r_a = g = \gamma$ and $\kappa/g = 0.001$.

$$\beta_{12} = \beta_{21})$$

$$\begin{aligned} \dot{\rho} = & -i\alpha(\rho a_1 a_2 - a_2 \rho a_1)e^{i\phi} - i\alpha(\rho a_1^\dagger a_2^\dagger - a_1^\dagger \rho a_2^\dagger)e^{-i\phi} \\ & + i\alpha(a_1 a_2 \rho - a_2 \rho a_1)e^{i\phi} + i\alpha(a_1^\dagger a_2^\dagger \rho - a_1^\dagger \rho a_2^\dagger)e^{-i\phi} \\ & - \kappa_1(a_1^\dagger a_1 \rho - 2a_1 \rho a_1^\dagger + \rho a_1^\dagger a_1) \\ & - \kappa_2(a_2^\dagger a_2 \rho - 2a_2 \rho a_2^\dagger + \rho a_2^\dagger a_2), \end{aligned} \quad (3.26)$$

This equation describes a parametric oscillator in the parametric approximation. We can calculate the time evolution of the quantum fluctuations of the EPR-operators \hat{u} and \hat{v} and the mean photon numbers from Eq. (3.26). In particular, we calculate the time evolution of the various moments involved in the quantities $(\Delta\hat{u})^2 + (\Delta\hat{v})^2$ and the total photon numbers $\langle\hat{N}\rangle = \langle\hat{N}_1\rangle + \langle\hat{N}_2\rangle$. The resulting expressions are

$$\begin{aligned} [(\Delta\hat{u})^2 + (\Delta\hat{v})^2](t) = & \{[(\Delta\hat{u})^2 + (\Delta\hat{v})^2](0) \\ & - \frac{2\kappa}{\alpha + \kappa}\}e^{-2(\alpha+\kappa)t} \\ & + \frac{2\kappa}{\alpha + \kappa} \end{aligned} \quad (3.27)$$

$$\begin{aligned} \langle\hat{N}\rangle(t) = & \left\{ \left(\langle\hat{N}\rangle(0) - \frac{\alpha^2}{\kappa^2 - \alpha^2} \right) \cosh(2\alpha t) \right. \\ & - \left(\frac{\alpha\kappa}{\kappa^2 - \alpha^2} + \langle a_1 a_2 + a_1^\dagger a_2^\dagger \rangle(0) \right) \sinh(2\alpha t) \Big\} \\ & \times e^{-2\kappa t} + \frac{\alpha^2}{\kappa^2 - \alpha^2}, \end{aligned} \quad (3.28)$$

where we have taken the phase of the driven field to be $\phi = -\pi/2$ since only under this special phase the positive exponential terms in $(\Delta\hat{u})^2 + (\Delta\hat{v})^2$ can be canceled out and ensure that this quantity does not grow with time.

It is clear that, for any initial state of the field, the quantity $(\Delta\hat{u})^2 + (\Delta\hat{v})^2$ becomes smaller as time evolves and becomes less than 2 after some time. For large

time when $(\alpha + \kappa)t \gg 1$, we have $(\Delta\hat{u})^2 + (\Delta\hat{v})^2 = 2\frac{\kappa}{\alpha+\kappa} < 2$, i.e., the entanglement criterion is satisfied. Thus the system evolves into an entangled state and remains entangled unless the entanglement is destroyed by some other dissipation channels. We show below that the results based on the parametric approximation are valid for small values of gt only and higher order contributions in γ/Ω tend to wipe out the entanglement as time progresses. Thus, for the general case, the entanglement remains only for a limited period of time.

The other important quantity is the mean number of photons in the two modes. If we consider the large time behavior of the total photon number, we can neglect the negative exponent terms in the sinh and cosh functions in Eq. (3.28). We then have $\langle\hat{N}\rangle(t) = [\langle\hat{N}\rangle(0) - \langle a_1a_2 + a_1^\dagger a_2^\dagger \rangle(0) + \alpha/(\alpha - \kappa)]\exp[2(\alpha - \kappa)t] - \alpha^2/(\alpha^2 - \kappa^2)$. This shows that, for any initial states of the two modes, the total mean photon number increases exponentially for sufficiently large t provided $\alpha > \kappa$. The condition for the growth of mean photon numbers for small t involves the initial states of the field. For example, for the initial coherent states $|\alpha_1\rangle$ and $|\alpha_2\rangle$ for the two modes, this will very much depends on the phase of the coherent amplitude of these two modes. The condition $d\langle\hat{N}\rangle(t)/dt > 0$, for $t \geq 0$, leads us to the following inequality $\alpha\langle a_1a_2 + a_1^\dagger a_2^\dagger \rangle(0) + \kappa\langle\hat{N}\rangle(0) < 0$ that is $\alpha(\alpha_1\alpha_2 + \alpha_1^*\alpha_2^*) + \kappa(|\alpha_1|^2 + |\alpha_2|^2) < 0$. To satisfy this inequality, the best choice is that, in addition to $\alpha > \kappa$, we also have $\alpha_1\alpha_2 = -|\alpha_1\alpha_2|$.

We now return to the general case. The various field moments required in the inequality (3.23) can be obtained from Eq. (3.18). The resulting expressions are complicated and we do not reproduce them here.

In Figs. 12 and 13 we show the time development of $(\Delta\hat{u})^2 + (\Delta\hat{v})^2$ and $\langle\hat{N}\rangle$ for different Ω/γ and fixed κ/g . In Fig. 12, we plot these quantities for an initial coherent state with 10^4 photons in each mode. The choice of the phase for the

coherent amplitude is such that the condition $\alpha_1\alpha_2 = -|\alpha_1\alpha_2|$ is satisfied. The parameter values are such that they correspond to the micromaser experiments in Garching [64]. We find that the two states remain entangled for a long time. The parametric results are valid only for $gt < 10$. The agreement between the parametric results with the exact results for the mean photon number $\langle\hat{N}\rangle$ is valid for a longer range. We also see that an increase in the photon numbers by almost 40 fold is possible. In Fig. 13, we plot $(\Delta\hat{u})^2 + (\Delta\hat{v})^2$ and $\langle\hat{N}\rangle$ for initial vacuum states for the two modes. Again, the entanglement is retained for a large number of photons. The time scale for the two modes to remain entangled increases as the Rabi frequency of the driving field is increased.

In summary, we have studied a cascade correlated emission laser system in which a macroscopic entangled state between two modes of the radiation field can be built. The entanglement does not depend on the initial state of the fields. Our analysis indicates that such macroscopic entangled states can be realized as suggested above by placing the atomic medium inside the doubly resonant cavity. Another possibility is a system wherein atoms with long lived states pass through the cavity one at a time such that there is at most one atom inside the cavity at a given time in the presence of the classical driving fields. This corresponds to experimental arrangements such as those used in the micromaser experiments [64, 65].

B. Entanglement generation in quantum beat lasers

In this section, we discuss the entanglement features of other CEL systems, such as quantum beat lasers [3].

Before we go into a detail discussion, another issue need to be addressed first. Let's consider a quantum beat laser that is pumped into its two upper levels $|a\rangle$ and

$|b\rangle$ with maximum coherence, the two laser modes are initially in vacuum states, and the initial state of this system can be described as $|\psi\rangle = \frac{1}{\sqrt{2}}(|a\rangle + |b\rangle)|0,0\rangle$. After one emission, the atom will go into its ground state $|c\rangle$ and the two laser modes will be maximally entangled. We have, after tracing out the atomic states, the state of the field is $|\psi_f\rangle = \frac{1}{\sqrt{2}}(|1,0\rangle + |0,1\rangle)$. What surprised us is that no physically measurable entanglement criteria that have been found can verify the entanglement for such a simple state. Great efforts have been put and lead us to find a new criterion, which is appropriate for testifying the entanglement of quantum beat systems [66].

In the following, we first introduce the new entanglement criterion. We then discuss the entanglement of a non-degenerate parametric converter as a simple application to this criterion. We conclude this section by the discussion of the entanglement of quantum beat lasers.

1. The entanglement criterion

This entanglement criterion involves calculations of the variances of two angular momentum type operators. It can be described as following: a state of a bipartite system is entangled if it satisfies the following inequality,

$$(\Delta L_1)^2 + (\Delta L_2)^2 < 2(\langle N_a \rangle + \langle N_b \rangle), \quad (3.29)$$

where, we define the following angular momentum type operators

$$\begin{aligned} L_1 &= ab^\dagger + a^\dagger b \\ L_2 &= i(ab^\dagger - a^\dagger b), \end{aligned} \quad (3.30)$$

a, b and a^\dagger, b^\dagger are the annihilation and creation operators of the two subsystems, and $N_a = a^\dagger a$ and $N_b = b^\dagger b$ are the photon number operators. The proof of this criterion is quite simple: We know that the density matrix of a separable state for a bipartite

system can be written as $\rho = \sum_i p_i \rho_i^{(A)} \times \rho_i^{(B)}$, where $p_i \geq 0$ and $\sum_i p_i = 1$. By plugging this density matrix into the left hand side of inequality (3.29), we have

$$(\Delta L_1)^2 + (\Delta L_2)^2 = \sum_i p_i ((\Delta L_1)_i^2 + (\Delta L_2)_i^2) \quad (3.31)$$

$$= 2 \sum_i p_i [\langle N_a + 1 \rangle_i \langle N_b \rangle_i + \langle N_a \rangle_i \langle N_b + 1 \rangle_i] \quad (3.32)$$

$$- 2 |\langle a \rangle_i \langle b^\dagger \rangle_i|^2 \quad (3.33)$$

$$\geq 2 \sum_i p_i [\langle N_a \rangle_i + \langle N_b \rangle_i] \quad (3.34)$$

$$\geq 2 [\langle N_a \rangle + \langle N_b \rangle]. \quad (3.35)$$

Here, $\langle \rangle_i$ means the expectation value with respect to the sub-species $\rho_i^{(A)} \times \rho_i^{(B)}$, and we have used

$$|\langle a \rangle|^2 \leq \langle N_a \rangle \quad (3.36)$$

and the Schwartz inequality in the last two steps. A family of similar entanglement conditions can be obtained based on this criterion. A detail discussion of this topic can be found in reference [66].

It is easy to verify that this criterion can detect the entanglement for the simple state $\frac{1}{\sqrt{2}}(|1, 0\rangle + |0, 1\rangle)$. We find that for this state,

$$(\Delta L_1)^2 + (\Delta L_2)^2 = 1 < 2(\langle N_a \rangle + \langle N_b \rangle) = 2. \quad (3.37)$$

We notice that the entanglement criterion (3.29) can actually be simplified, since we have

$$(\Delta L_1)^2 + (\Delta L_2)^2 - 2(\langle N_a \rangle + \langle N_b \rangle) = \langle N_1 N_2 \rangle - |\langle a_1^\dagger a_2 \rangle|^2. \quad (3.38)$$

We then can also use the following equivalent inequality to testify the entanglement,

$$\langle N_1 N_2 \rangle - |\langle a_1^\dagger a_2 \rangle|^2 < 0. \quad (3.39)$$

2. Entanglement production of non-degenerate parametric converters

Prepared by the entanglement criterion, let us now demonstrate some applications. A simple application of this criterion would be a non-degenerate parametric converter. Analogous to the parametric down conversion oscillator, we define a system which has the following Hamiltonian

$$H = \hbar\epsilon(a_1^\dagger a_2 e^{i\phi} + a_2^\dagger a_1 e^{-i\phi}) \quad (3.40)$$

as non-degenerate parametric converter, where ϵ and ϕ are the intensity and phase of the effective pumping field. We see that instead of a sum-frequency transition in a parametric down conversion oscillator, we have a sub-frequency transition for this system. We believe this system can be implemented by using some kind of non-linear crystals. The equations of motion for the two field mode operators in the Heisenberg picture are,

$$\begin{aligned} \dot{a}_1(t) &= -i\epsilon a_2(t) e^{i\phi}, \\ \dot{a}_2(t) &= -i\epsilon a_1(t) e^{-i\phi}. \end{aligned} \quad (3.41)$$

The solutions of these equations are given by

$$\begin{aligned} a_1(t) &= a_1(0) \cos(\epsilon t) - i a_2(0) e^{i\phi} \sin(\epsilon t), \\ a_2(t) &= a_2(0) \cos(\epsilon t) - i a_1(0) e^{i\phi} \sin(\epsilon t). \end{aligned} \quad (3.42)$$

The various momenta of the field operators required in calculations of inequality (3.39) can then be computed provided with the initial state of the field. If the initial state of the field is a Fock-state $|\psi\rangle = |n_1, n_2\rangle$ (n_1 and n_2 are initial photon numbers

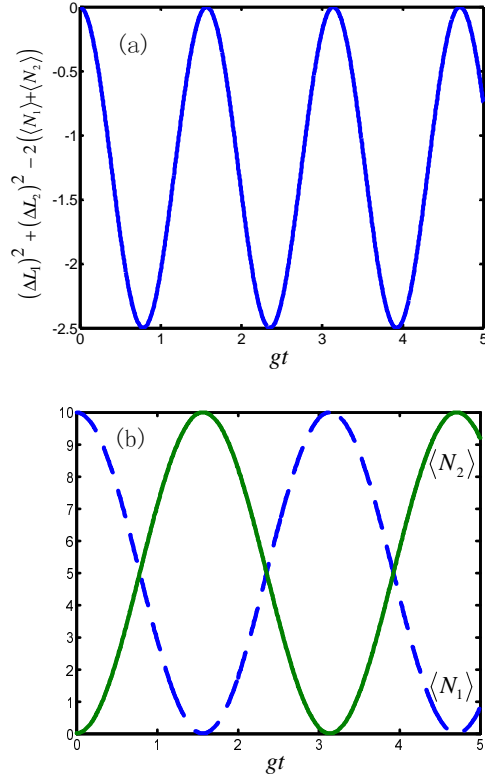


Fig. 14. The entanglement(a) and photon numbers(b) (the dash line is for mode 1 and the solid line is for mode 2) of a parametric quantum beat oscillator, we take $\epsilon = 1$ and the initial state of the field being $|10, 0\rangle$ for a special case.

of the two field modes), we obtain

$$\langle a_1^\dagger a_2 \rangle = ie^{-i\phi} SC(n_2 - n_1), \quad (3.43)$$

$$\langle N_1 N_2 \rangle = n_1 n_2 (C^4 + S^4) + [(n_2 - n_1)^2 - (n_1 + n_2)] S^2 C^2, \quad (3.44)$$

where $C = \cos(\epsilon t)$ and $S = \sin(\epsilon t)$. We then have for the left hand side of inequality (3.39)

$$\langle N_1 N_2 \rangle - |\langle a_1^\dagger a_2 \rangle|^2 = n_1 n_2 (C^4 + S^4) - (n_1 + n_2) C^2 S^2. \quad (3.45)$$

The requirement of the entanglement being detected all the time by the criterion

(3.39) lead us to having either $n_1 = 0$ and $n_2 \neq 0$ or $n_2 = 0$ and $n_1 \neq 0$. This means that one of the field modes is initially in vacuum state. Fig. 14 shows the result for the initial state of the field being $|10, 0\rangle$. We see that there are oscillations in the photon numbers as well as in the the left hand side of inequality (3.39). We see that the left hand side of inequality (3.39) are always negative, which hints the two field modes are always entangled.

3. Field entanglement in a quantum beat laser

We now discuss the entanglement production in a quantum beat laser. A quantum beat laser contains a ‘V’-type atomic system inside a doubly resonant cavity (see Fig. 15). Atoms are prepared in a coherent superposition of upper levels $|a\rangle$ and $|b\rangle$ by an external classical field with an effective Rabi frequency $\Omega e^{-i\phi}$. The two laser transitions $|a\rangle - |c\rangle$ and $|b\rangle - |c\rangle$ with frequencies ν_1 and ν_2 share a common lower level $|c\rangle$. The Hamiltonian for this system in the interaction picture and under the dipole approximation and rotating wave approximation is given by

$$V = \hbar g(a_1 e^{i\Delta t}|a\rangle\langle c| + a_2 e^{i\Delta t}|b\rangle\langle c| - \frac{\hbar\Omega}{2}e^{-i\phi}|a\rangle\langle b| + H.c.), \quad (3.46)$$

where we have assumed the common atom field coupling constant g for mode 1 and 2. $\Delta = \omega_a - \omega_c - \nu_1 = \omega_b - \omega_c - \nu_2$ is the atomic detuning with respect to the field. For simplicity, we have assumed the classical driving field has a frequency of $\nu_3 = \omega_{ab}$. The master equation of this system can be derived under the linear approximation

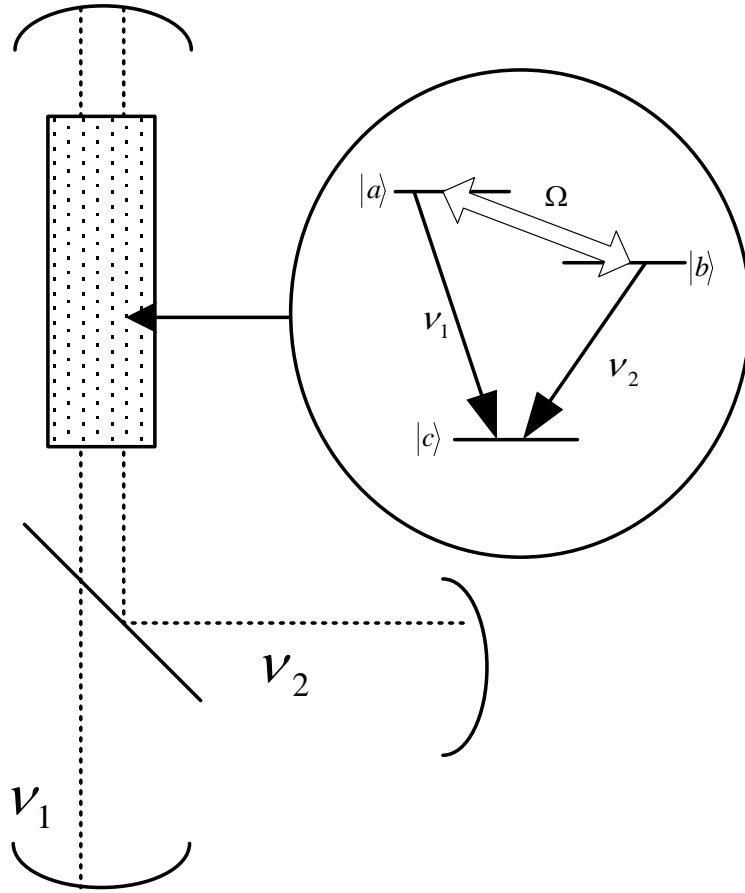


Fig. 15. A schematic of the system setup for a quantum beat laser

by keeping the coupling constant g to its first order [67],

$$\begin{aligned}
\dot{\rho} = & -\frac{1}{2}\alpha_{11}(\rho a_1 a_1^\dagger - a_1^\dagger \rho a_1) - \frac{1}{2}\alpha_{22}(\rho a_2 a_2^\dagger - a_2^\dagger \rho a_2) \\
& - \frac{1}{2}\alpha_{12}(\rho a_2 a_1^\dagger - a_1^\dagger \rho a_2)e^{i\phi} \\
& - \frac{1}{2}\alpha_{21}(\rho a_1 a_2^\dagger - a_2^\dagger \rho a_1)e^{-i\phi} + H.c. \\
& - \frac{\kappa_1}{2}(a_1^\dagger a_1 \rho - 2a_1 \rho a_1^\dagger + \rho a_1^\dagger a_1) \\
& - \frac{\kappa_2}{2}(a_2^\dagger a_2 \rho - 2a_2 \rho a_2^\dagger + \rho a_2^\dagger a_2),
\end{aligned} \tag{3.47}$$

where

$$\begin{aligned}
\alpha_{11} = & \frac{g^2 r_a}{2\gamma(\gamma^2 + \Omega^2)} \left\{ \frac{(2\gamma^2 + \Omega^2 + i\Omega\gamma)[\gamma - i(\Delta - \Omega/2)]}{\gamma^2 + (\Delta - \Omega/2)^2} \right. \\
& \left. + \frac{(2\gamma^2 + \Omega^2 - i\Omega\gamma)[\gamma - i(\Delta + \Omega/2)]}{\gamma^2 + (\Delta + \Omega/2)^2} \right\},
\end{aligned} \tag{3.48}$$

$$\begin{aligned}
\alpha_{12} = & \frac{g^2 r_a \Omega}{2\gamma(\gamma^2 + \Omega^2)} \left\{ \frac{\gamma - i(\Delta - \Omega/2)}{\gamma^2 + (\Delta - \Omega/2)^2}(\Omega - i\gamma) \right. \\
& \left. - \frac{\gamma - i(\Delta + \Omega/2)}{\gamma^2 + (\Delta + \Omega/2)^2}(\Omega + i\gamma) \right\},
\end{aligned} \tag{3.49}$$

$$\begin{aligned}
\alpha_{21} = & \frac{g^2 r_a}{2\gamma(\gamma^2 + \Omega^2)} \left\{ \frac{(2\gamma^2 + \Omega^2 + i\Omega\gamma)[\gamma - i(\Delta - \Omega/2)]}{\gamma^2 + (\Delta - \Omega/2)^2} \right. \\
& \left. - \frac{(2\gamma^2 + \Omega^2 - i\Omega\gamma)[\gamma - i(\Delta + \Omega/2)]}{\gamma^2 + (\Delta + \Omega/2)^2} \right\},
\end{aligned} \tag{3.50}$$

$$\begin{aligned}
\alpha_{22} = & \frac{g^2 r_a \Omega}{2\gamma(\gamma^2 + \Omega^2)} \left\{ \frac{\gamma - i(\Delta - \Omega/2)}{\gamma^2 + (\Delta - \Omega/2)^2}(\Omega - i\gamma) \right. \\
& \left. + \frac{\gamma - i(\Delta + \Omega/2)}{\gamma^2 + (\Delta + \Omega/2)^2}(\Omega + i\gamma) \right\}.
\end{aligned} \tag{3.51}$$

We have assumed here atoms are injected into their upper levels $|a\rangle$ at a rate r_a . Note here, we have included the cavity decays by assuming that the two laser modes damp through two vacuum reservoirs independently. κ_1 and κ_2 are then the two cavity damping rates. Atomic decays have also been phenomenologically introduced and we assume all three levels have the common atomic decay rate γ . Here the terms

proportional to α_{11} and α_{22} are the gain terms, which correspond to the emission from level $|a\rangle$ and $|c\rangle$, respectively. These processes are noncoherent processes and they will wipe out the entanglement if they exist. The terms proportional to β_{12} and β_{21} correspond to atomic coherence generated by the coupling field Ω . These terms describe the process where one photon is absorbed and another photon in the other cavity mode is emitted and these are the entanglement source terms. However, we see that there is no gain associated with this coherent process. As a result, an amplified entangled field is not obtained in a quantum beat laser. This is not like the cascade CEL where two photons are coherently emitted and thus the coherence terms can also provide gains to the field [68].

We notice here, if we assume $\Omega \rightarrow \infty$ and ignore all cavity dampings, that is $\kappa_1 = \kappa_2 = 0$ and keep $1/\Omega$ to its first order, we will have for Eqs. (3.48-3.51)

$$\alpha_{11} \approx \alpha_{22} \approx 0, \alpha_{12} \approx \alpha_{21} \approx \frac{2ig^2r_a}{\gamma\Omega}. \quad (3.52)$$

We thus approximately ignored the noncoherent amplification terms. The master equation (3.47) can be simplified as

$$\dot{\rho} = i\epsilon[(\rho a_2 a_1^\dagger - a_1^\dagger \rho a_2)e^{i\phi} + (\rho a_1 a_2^\dagger - a_2^\dagger \rho a_1)e^{-i\phi}] + H.c., \quad (3.53)$$

where $\epsilon = \frac{i}{2}\alpha_{12} = -\frac{g^2r_a}{\gamma\Omega}$. This master equation exactly describes a non-degenerate parametric converter that we have discussed in the previous section. The calculation for the general case with considerations of cavity dampings and limited Ω effects is rather tedious so that we didn't duplicate it here. The results are shown in Fig. (16). As we have just discussed, we see that the noncoherent cavity damping terms and gain terms will wipe out the entanglement of the field modes. The entanglement can only be observed for states with small number of photons.

In a summary, we have discussed the entanglement features of non-degenerate

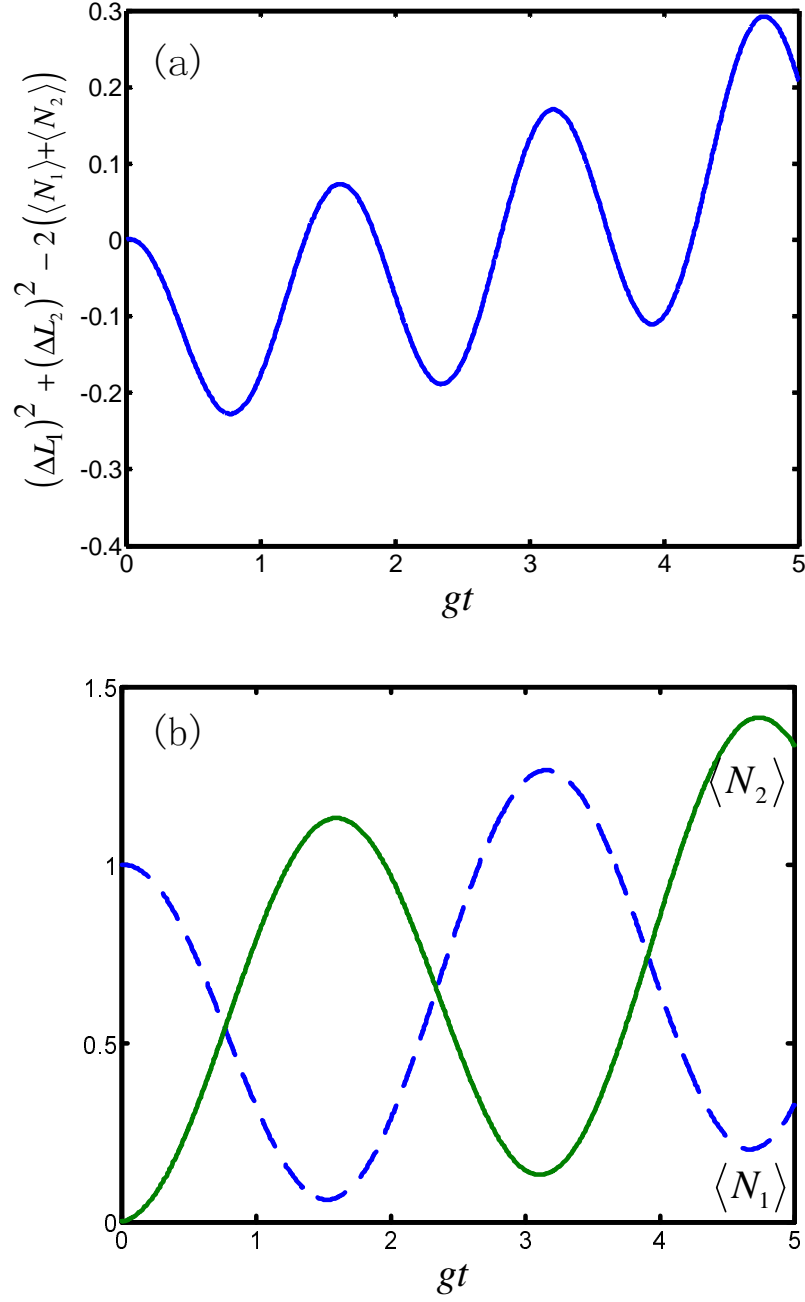


Fig. 16. The time evolution of entanglement(a) and photon numbers(b)(the dash line is for mode 1 and the solid line is for mode 2) of a quantum beat laser. The following parameters have been chosen: $r_a = 1$, $\Omega = 10$, $\gamma = 0.1$, $g = 1$, $\Delta = 0$ and $\phi = \pi$.

parametric converters and quantum beat lasers. A new entanglement criterion has been applied to verify the entanglement in those systems. We claim that entanglement can be produced when one of the field mode is initially in vacuum state and the other field mode is initially prepared in a Fock-state. This entanglement can only be observed for states with small number of photons.

CHAPTER IV

NON-DEGENERATE PARAMETRIC AMPLIFIER AS AN ENTANGLEMENT SOURCE

We have seen that the entanglement amplifier we just discussed in the previous section becomes into a Non-degenerate parametric amplifier (NOPA) when the classical pumping field is much larger than the atomic decay rate. In this chapter we are going to discuss the entanglement generation of NOPA systems in detail. We especially carry out the input-output calculations of a NOPA and to show that the two output fields of a NOPA are still entangled. We also consider the effects of the pumping fluctuations on the entanglement generation of NOPA systems in this chapter.

A. The entanglement of an NOPA: below and above the threshold

1. System description and the Hamiltonian

We consider a system with a type II nonlinear crystal placed in an optical cavity tuned to allow three modes of the light field of frequencies ω_1 , ω_2 and ω_3 with $\omega_1 + \omega_2 = \omega_3$ as shown in Fig. 17. Here, mode 3 is pumped by some external laser field at frequency ω_3 and modes 1 and 2 are the signal and idler modes of the NOPO. These three modes (modes 1, 2 and 3) are in contact with three bathes (bath 1, bath 2 and bath 3) through some semitransparent mirrors. The total Hamiltonian of this system can be written as

$$\begin{aligned}
 H_{tot} = & H_{sys} + H_{pump} + H_{bath1} + H_{int1} + H_{bath2} + H_{int2} \\
 & + H_{bath3} + H_{int3},
 \end{aligned}
 \tag{4.1}$$

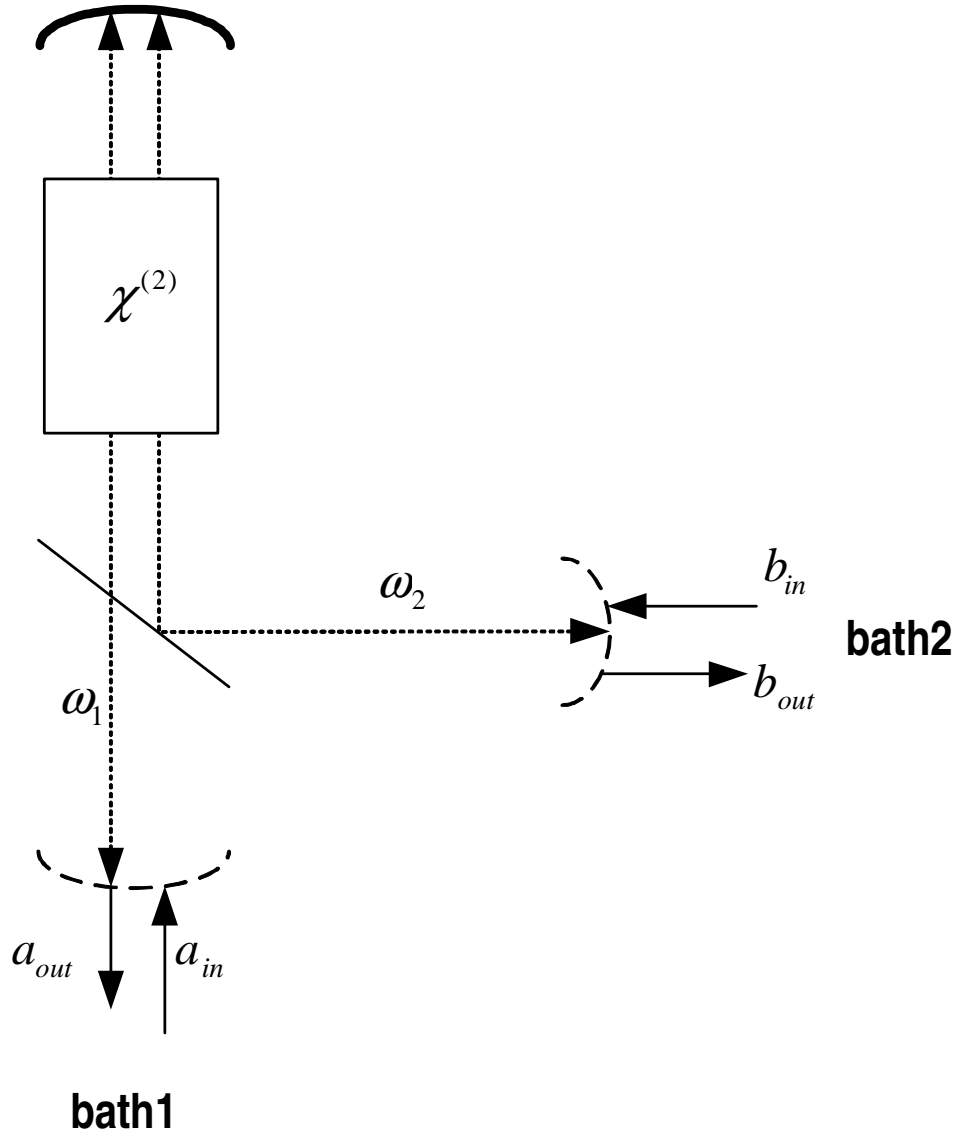


Fig. 17. A scheme for our non-degenerate parametric oscillator system. It consists of a type II crystal located in an optical cavity tuned to allow three modes of the light field of frequencies ω_1 , ω_2 and ω_3 with $\omega_1 + \omega_2 = \omega_3$. Mode 3 is pumped by an external laser at frequency ω_3 . Modes 1 and 2 are the signal and idler modes of this oscillator that interact with two baths (bath 1 and bath 2), with $a_{in}(b_{in})$ and $a_{out}(b_{out})$ to be the input and output fields of bath 1 (bath 2).

where H_{sys} depends only on the internal modes operators. H_{pump} describes the external laser pumping of mode 3. H_{bath1} , H_{bath2} and H_{bath3} are the free Hamiltonians for bath 1, 2 and 3, respectively. H_{int1} describes the interaction between cavity mode 1 and bath 1 and so do H_{int2} and H_{int3} . For a nondegenerate parametric oscillator system, H_{sys} can be written as

$$H_{sys} = \hbar\omega_1 a_1^\dagger a_1 + \hbar\omega_2 a_2^\dagger a_2 + \hbar\omega_3 a_3^\dagger a_3 + \frac{1}{2}i\hbar g[a_1^\dagger a_2^\dagger a_3 - a_1 a_2 a_3^\dagger], \quad (4.2)$$

where a_1 , a_2 , a_3 and a_1^\dagger , a_2^\dagger , a_3^\dagger are the annihilation and creation operators for the cavity modes 1, 2 and 3. g describes the nonlinear coupling due to the type II nonlinear crystal. The pumping hamiltonian of mode 3 can be written as

$$H_{pump} = i\hbar[Ea_3^\dagger \exp(-i\omega_3 t) - E^* a_3 \exp(i\omega_3 t)], \quad (4.3)$$

where E is the complex amplitude of the driving laser field. The rest terms describe the time irreversible damping of these cavity fields and can be treated by some traditional methods [69].

2. Input and output calculations: below the threshold

Let's first consider the case when the system operates below its threshold. For this case, we can treat the third mode field classically and represent all the effects due to this field by a classical effective pumping field to the nonlinear crystal inside the cavity. Under this consideration, we simply ignore the external pumping and the cavity damping associated with mode 3, and the Hamiltonian becomes

$$H_{tot} = H_{sys} + H_{bath1} + H_{int1} + H_{bath2} + H_{int2}, \quad (4.4)$$

and

$$H_{sys} = \hbar\omega_1 a_1^\dagger a_1 + \hbar\omega_2 a_2^\dagger a_2 + \frac{1}{2}i\hbar[\epsilon e^{-i\omega_3 t} a_1^\dagger a_2^\dagger - \epsilon^* e^{i\omega_3 t} a_1 a_2], \quad (4.5)$$

where ϵ is the effective pump intensity, which could be a complex number.

Following Gardiner's input-output theory for quantum dissipative systems [69], we use the Hamiltonian (4.4) to obtain quantum Langevin equations for those cavity modes

$$\frac{da_1}{dt} = -\frac{i}{\hbar}[a_1, H_{sys}] - \frac{\gamma_1}{2}a_1 + \sqrt{\gamma_1}a_{in} \quad (4.6)$$

$$= -\frac{i}{\hbar}[a_1, H_{sys}] + \frac{\gamma_1}{2}a_1 - \sqrt{\gamma_1}a_{out} \quad (4.7)$$

$$\frac{da_2}{dt} = -\frac{i}{\hbar}[a_2, H_{sys}] - \frac{\gamma_2}{2}a_2 + \sqrt{\gamma_2}b_{in} \quad (4.8)$$

$$= -\frac{i}{\hbar}[a_2, H_{sys}] + \frac{\gamma_2}{2}a_2 - \sqrt{\gamma_2}b_{out}, \quad (4.9)$$

where γ_1 and γ_2 are the cavity damping rates for mode 1 and 2 and $\sqrt{\gamma_1}a_{in}$, $\sqrt{\gamma_1}a_{out}$, $\sqrt{\gamma_2}b_{in}$ and $\sqrt{\gamma_2}b_{out}$ are the associated quantum noises with a_{in} , a_{out} and b_{in} , b_{out} to be the incoming and outcoming parts of the external fields for bath 1 and bath 2, respectively. We can then substitute in the H_{sys} for the nondegenerate parametric oscillator and obtain

$$\frac{da_1}{dt} = -i\omega_1 a_1 + \frac{1}{2}\epsilon e^{-i\omega_3 t} a_2^\dagger - \frac{\gamma_1}{2}a_1 + \sqrt{\gamma_1}a_{in} \quad (4.10)$$

$$= -i\omega_1 a_1 + \frac{1}{2}\epsilon e^{-i\omega_3 t} a_2^\dagger + \frac{\gamma_1}{2}a_1 - \sqrt{\gamma_1}a_{out} \quad (4.11)$$

$$\frac{da_2}{dt} = -i\omega_2 a_2 + \frac{1}{2}\epsilon e^{-i\omega_3 t} a_1^\dagger - \frac{\gamma_2}{2}a_2 + \sqrt{\gamma_2}b_{in} \quad (4.12)$$

$$= -i\omega_2 a_2 + \frac{1}{2}\epsilon e^{-i\omega_3 t} a_1^\dagger + \frac{\gamma_2}{2}a_2 - \sqrt{\gamma_2}b_{out}. \quad (4.13)$$

In the rotating frame

$$a_1 = \bar{a}_1 e^{-i\omega_1 t} a_{in} = \bar{a}_{in} e^{-i\omega_1 t}$$

$$a_2 = \bar{a}_2 e^{-i\omega_2 t} b_{in} = \bar{b}_{in} e^{-i\omega_2 t}.$$

If assuming $\gamma = \gamma_1 = \gamma_2$, we obtain

$$\frac{d\bar{a}_1}{dt} = \frac{1}{2}\epsilon\bar{a}_2^\dagger - \frac{\gamma}{2}\bar{a}_1 + \sqrt{\gamma}\bar{a}_{in} = \frac{1}{2}\epsilon\bar{a}_2^\dagger + \frac{\gamma}{2}\bar{a}_1 - \sqrt{\gamma}\bar{a}_{out}, \quad (4.14)$$

$$\frac{d\bar{a}_2}{dt} = \frac{1}{2}\epsilon\bar{a}_1^\dagger - \frac{\gamma}{2}\bar{a}_1 + \sqrt{\gamma}\bar{b}_{in} = \frac{1}{2}\epsilon\bar{a}_1^\dagger + \frac{\gamma}{2}\bar{a}_2 - \sqrt{\gamma}\bar{b}_{out}. \quad (4.15)$$

The above equations can be written in matrix form as

$$\frac{d\mathbf{a}}{dt} = (\mathbf{A} - \frac{\gamma}{2}\mathbf{I}) \cdot \mathbf{a} + \sqrt{\gamma}\mathbf{a}_{in} \quad (4.16)$$

$$= (\mathbf{A} + \frac{\gamma}{2}\mathbf{I}) \cdot \mathbf{a} - \sqrt{\gamma}\mathbf{a}_{out}, \quad (4.17)$$

where \mathbf{A} is a matrix and

$$\mathbf{A} = \begin{pmatrix} 0 & 0 & 0 & \frac{1}{2}\epsilon \\ 0 & 0 & \frac{1}{2}\epsilon^* & 0 \\ 0 & \frac{1}{2}\epsilon & 0 & 0 \\ \frac{1}{2}\epsilon^* & 0 & 0 & 0 \end{pmatrix}, \quad \mathbf{a} = \begin{pmatrix} \bar{a}_1 \\ \bar{a}_1^\dagger \\ \bar{a}_2 \\ \bar{a}_2^\dagger \end{pmatrix}. \quad (4.18)$$

It is appropriate to consider the solution in the frequency domain. Therefore, we do the following Fourier transform

$$\bar{a}(t) = \frac{1}{\sqrt{2\pi}} \int_{-\infty}^{\infty} e^{-i\omega t} \tilde{a}(\omega) d\omega. \quad (4.19)$$

Equation (4.16) then becomes

$$-i\omega\tilde{\mathbf{a}}(\omega) = (\mathbf{A} - \frac{\gamma}{2}\mathbf{I}) \cdot \tilde{\mathbf{a}}(\omega) + \sqrt{\gamma}\tilde{\mathbf{a}}_{in}(\omega) \quad (4.20)$$

$$= (\mathbf{A} + \frac{\gamma}{2}\mathbf{I}) \cdot \tilde{\mathbf{a}}(\omega) - \sqrt{\gamma}\tilde{\mathbf{a}}_{out}(\omega), \quad (4.21)$$

where

$$\underline{\tilde{a}}(\omega) = \begin{pmatrix} \tilde{a}_1(\omega) \\ \tilde{a}_1^\dagger(-\omega) \\ \tilde{a}_2(\omega) \\ \tilde{a}_2^\dagger(-\omega) \end{pmatrix}. \quad (4.22)$$

We are only concerned about the steady state result here. Therefore while taking the Fourier transform of the first derivative of $\underline{a}(t)$ in Eq. (4.10), we simply ignore the term depending on the initial condition $\underline{a}(0)$, since this term contributes only to the transient behavior. For simplicity, we assume all integrals over frequency in those fourier transforms extend over an interval large compared to the cavity bandwidth but small compared to the actual central frequencies ω_1 and ω_2 . With this assumption, we can prove that the annihilation and creation operators in the frequency domain obey the following commutation relation

$$[\tilde{a}_{in}(\omega), \tilde{a}_{in}(\omega')] = 0 \quad [\tilde{a}_{in}(\omega), \tilde{a}_{in}^\dagger(\omega')] = \delta(\omega - \omega') \quad (4.23)$$

$$[\tilde{b}_{in}(\omega), \tilde{b}_{in}(\omega')] = 0 \quad [\tilde{b}_{in}(\omega), \tilde{b}_{in}^\dagger(\omega')] = \delta(\omega - \omega'). \quad (4.24)$$

We can eliminate the operators for the internal modes $\underline{\tilde{a}}(\omega)$ and express the output field operators in terms of the input field operators as

$$\underline{\tilde{a}}_{out}(\omega) = [\mathbf{A} + (\frac{\gamma}{2} + i\omega)\mathbf{I}][-\mathbf{A} + (\frac{\gamma}{2} - i\omega)\mathbf{I}]^{-1}\underline{\tilde{a}}_{in}(\omega). \quad (4.25)$$

We then evaluate all those matrices and multiply the right hand side of Eq. (4.25).

After some transformations and calculations, we obtain

$$\tilde{a}_{out}(\omega_1 + \omega) = \frac{1}{D} [C_1 \tilde{a}_{in}(\omega_1 + \omega) + C_2 \tilde{b}_{in}^\dagger(\omega_2 - \omega)] \quad (4.26)$$

$$\tilde{a}_{out}^\dagger(\omega_1 + \omega) = \frac{1}{D^*} [C_1 \tilde{a}_{in}^\dagger(\omega_1 + \omega) + C_2^* \tilde{b}_{in}(\omega_2 - \omega)] \quad (4.27)$$

$$\tilde{b}_{out}(\omega_2 - \omega) = \frac{1}{D^*} [C_1 \tilde{b}_{in}(\omega_1 - \omega) + C_2 \tilde{a}_{in}^\dagger(\omega_1 + \omega)] \quad (4.28)$$

$$\tilde{b}_{out}^\dagger(\omega_2 - \omega) = \frac{1}{D} [C_1 \tilde{b}_{in}^\dagger(\omega_2 - \omega) + C_2^* \tilde{a}_{in}(\omega_1 + \omega)], \quad (4.29)$$

where $D = (\frac{\gamma}{2} - i\omega)^2 - \frac{|\epsilon|^2}{4}$ and $C_1 = \frac{\gamma^2 + |\epsilon|^2}{4} + \omega^2$, $C_2 = \frac{\gamma\epsilon}{2}$. We note that we have allowed the rotation and changed back to the original frame from the rotating frame.

We recall that for the input fields are vacuum states, their normally ordered variance will all be zero, that is

$$\langle c, d \rangle = \langle c^\dagger, d \rangle = \langle c^\dagger, d^\dagger \rangle = 0, \quad (4.30)$$

where

$$\langle c, d \rangle = \langle cd \rangle - \langle c \rangle \langle d \rangle.$$

and c, d denotes either \tilde{a}_{in} or \tilde{b}_{in} . Under this condition, the only contribution to the normally ordered variance of the output fields will be from the commutator terms. This gives

$$\begin{aligned} & \langle \tilde{a}_{out}^\dagger(\omega_1 + \omega), \tilde{a}_{out}(\omega_1 + \omega') \rangle \\ &= \langle \tilde{b}_{out}^\dagger(\omega_2 - \omega), \tilde{b}_{out}(\omega_2 - \omega') \rangle \\ &= \left(\frac{\gamma|\epsilon|}{2|D|} \right)^2 \delta(\omega - \omega'), \end{aligned} \quad (4.31)$$

$$\begin{aligned} & \langle \tilde{a}_{out}(\omega_1 + \omega), \tilde{b}_{out}(\omega_2 - \omega') \rangle \\ &= \langle \tilde{b}_{out}^\dagger(\omega_2 - \omega), \tilde{a}_{out}^\dagger(\omega_1 + \omega') \rangle^* \\ &= \frac{\gamma\epsilon}{2|D|^2} \left(\frac{\gamma^2 + |\epsilon|^2}{4} + \omega^2 \right) \delta(\omega - \omega'). \end{aligned} \quad (4.32)$$

To estimate the entanglement for the output field, we adjust the entanglement criterion (3.23) and apply it in the frequency domain (one can easily verify this is applicable). We thus only care about the spectrum when we estimate the entanglement of the output field, the delta functions can then be ignored and we have, for the output field,

$$\begin{aligned}
& [(\Delta \hat{u}_{out})^2 + (\Delta \hat{v}_{out})^2]_\omega \\
&= 2[\langle \tilde{a}_{out}^\dagger, \tilde{a}_{out} \rangle + \langle \tilde{b}_{out}^\dagger, \tilde{b}_{out} \rangle + \langle \tilde{a}_{out}, \tilde{b}_{out} \rangle + \langle \tilde{b}_{out}^\dagger, \tilde{a}_{out}^\dagger \rangle]_\omega + 2 \\
&= \frac{1}{|D|^2} [\gamma^2 |\epsilon|^2 + \gamma(\epsilon + \epsilon^*) (\frac{\gamma^2 + |\epsilon|^2}{4} + \omega^2)] + 2.
\end{aligned} \tag{4.33}$$

Here ω is the frequency deviation from the central frequency. The associated frequencies with operators \tilde{a}_{out} , \tilde{a}_{out}^\dagger and \tilde{b}_{out} , \tilde{b}_{out}^\dagger are $\omega_1 + \omega$ and $\omega_2 - \omega$, respectively. The quantity $[(\Delta \hat{u}_{out})^2 + (\Delta \hat{v}_{out})^2]_\omega$ is less than 2 only if the real part of the effective pumping intensity $Re(\epsilon)$ is negative. An extreme case would be if ϵ is a negative real number, namely $\epsilon = -|\epsilon|$. Under this condition, we have

$$\begin{aligned}
& [(\Delta \hat{u}_{out})^2 + (\Delta \hat{v}_{out})^2]_\omega \\
&= \frac{1}{|D|^2} [\gamma^2 |\epsilon|^2 - 2\gamma |\epsilon| (\frac{\gamma^2 + |\epsilon|^2}{4} + \omega^2)] + 2 \\
&= 2 - \frac{8\gamma |\epsilon| [(\gamma - |\epsilon|)^2 + 4\omega^2]}{(\gamma^2 - |\epsilon|^2 - 4\omega^2)^2 + (4\gamma\omega)^2}.
\end{aligned} \tag{4.34}$$

Thus $[(\Delta \hat{u}_{out})^2 + (\Delta \hat{v}_{out})^2]_\omega$ is clearly smaller than 2 and the two modes ($\tilde{a}_{out}(\omega_1 + \omega)$ and $\tilde{b}_{out}(\omega_2 - \omega)$) of the output field are in an entangled state. At the central frequencies when $\omega = 0$ we have

$$[(\Delta \hat{u}_{out})^2 + (\Delta \hat{v}_{out})^2]_{\omega=0} = 2 - \frac{8\gamma |\epsilon|}{(\gamma + |\epsilon|)^2}. \tag{4.35}$$

This result is consistent with the result when we consider the entanglement for the intracavity modes in the previous section [68].

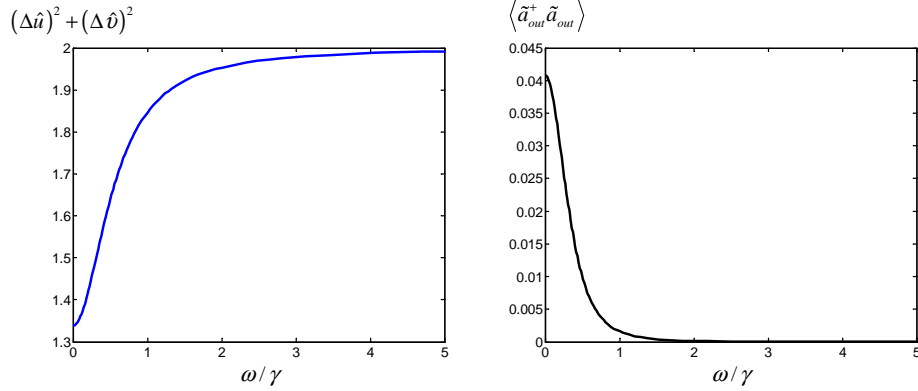


Fig. 18. Dependences of spectrum of the quantum fluctuations of EPR-like operators and intensities on the dimensionless frequency shift ω/γ , for system operating below the threshold $|\epsilon/\gamma| = 0.1$.

Another quantity we are concerned about is the intensity spectrum of these two entangled modes. Under the entanglement condition, i.e., $\epsilon = -|\epsilon|$ is a negative real number, we have

$$\begin{aligned} \langle \tilde{a}_{out}^\dagger \tilde{a}_{out} \rangle_\omega &= \langle \tilde{b}_{out}^\dagger \tilde{b}_{out} \rangle_\omega = \frac{\gamma^2 |\epsilon|^2}{4|D|^2} \\ &= \frac{4\gamma^2 |\epsilon|^2}{(\gamma^2 - |\epsilon|^2 - 4\omega^2)^2 + (4\gamma\omega)^2}. \end{aligned} \quad (4.36)$$

At the central frequencies, we have

$$\langle \tilde{a}_{out}^\dagger \tilde{a}_{out} \rangle_{\omega=0} = \langle \tilde{b}_{out}^\dagger \tilde{b}_{out} \rangle_{\omega=0} = \frac{4\gamma^2 |\epsilon|^2}{(\gamma^2 - |\epsilon|^2)^2}. \quad (4.37)$$

In Fig. 18, we see the dependence of the spectrum of the summation of quantum fluctuations of the EPR-like operators and the intensities on the dimensionless frequency shift ω/γ when the system operates below threshold. We see that the maximum entanglement as well as the maximum photon numbers happens at the center frequency $\omega/\gamma = 0$. They decrease monotonically with the increase of the frequency

shift ω/γ .

3. Input and output calculations: above the threshold

When the system operates above the threshold, we have to treat all intracavity field modes quantum mechanically. If we try to follow the input-output formulism in the previous section, we have to deal with some nonlinear Quantum Langevin Equations or some equivalent Quantum Stochastic Differential Equations for the intracavity field. It is well known from the regular Laser theory that a linearization technique is inapplicable due to the phase diffusion processes in this system. Phase space method is a typical way to solve this problem. In the following, we will follow the procedure proposed in reference [70] to obtain the required momenta for the intracavity field. We can then obtain the entanglement measure of the output field through the boundary conditions.

A summarization of this procedure is given in follows. By introducing the positive P representation, one can convert the master equation satisfied by the density operator $\hat{\rho}$ into a c-number Focker-Plank equation and then transformed into equivalent c-number stochastic differential equations,

$$\begin{aligned}
\dot{\alpha}_1 &= -\frac{\gamma}{2}\alpha_1 + g\alpha_3\alpha_2^\dagger + (g\alpha_3)^{1/2}\xi_1(t), \\
\dot{\alpha}_2 &= -\frac{\gamma}{2}\alpha_2 + g\alpha_3\alpha_1^\dagger + (g\alpha_3)^{1/2}\xi_2(t), \\
\dot{\alpha}_3 &= E - \frac{\gamma_3}{2}\alpha_3 - g\alpha_1\alpha_2, \\
\dot{\alpha}_1^\dagger &= -\frac{\gamma}{2}\alpha_1^\dagger + g\alpha_3^\dagger\alpha_2 + (g\alpha_3^\dagger)^{1/2}\xi_1^\dagger(t), \\
\dot{\alpha}_2^\dagger &= -\frac{\gamma}{2}\alpha_2^\dagger + g\alpha_3^\dagger\alpha_1 + (g\alpha_3^\dagger)^{1/2}\xi_2^\dagger(t), \\
\dot{\alpha}_3^\dagger &= E^* - \frac{\gamma_3}{2}\alpha_3^\dagger - g\alpha_1^\dagger\alpha_2^\dagger,
\end{aligned} \tag{4.38}$$

with $\xi(t)$ and $\xi^\dagger(t)$ the independent real white noise and have the following nonzero correlations,

$$\begin{aligned}\langle \xi_1(t)\xi_2(t') \rangle &= \delta(t - t') \\ \langle \xi_1^\dagger(t)\xi_2^\dagger(t') \rangle &= \delta(t - t').\end{aligned}$$

In order to deal with the phase diffusion process, we define the following phase and amplitude variables:

$$\begin{aligned}I_j &= \alpha_j^\dagger \alpha_j, \\ \phi_j &= \ln(\alpha_j^\dagger / \alpha_j) / 2i, j = 1, 2, 3.\end{aligned}\tag{4.39}$$

In terms of these variables, equation (4.38) can be transformed into

$$\begin{aligned}\dot{I}_1 &= -\gamma I_1 + 2g(I_1 I_2 I_3)^{1/2} \cos \psi + F_1(t), \\ \dot{\phi}_1 &= -g(I_2 I_3 / I_1)^{1/2} \sin \psi + f_1(t), \\ \dot{I}_2 &= -\gamma I_2 + 2g(I_1 I_2 I_3)^{1/2} \cos \psi + F_2(t), \\ \dot{\phi}_2 &= -g(I_1 I_3 / I_2)^{1/2} \sin \psi + f_2(t), \\ \dot{I}_3 &= 2|E|I_3^{1/2} \cos(\phi_3 - \phi_0) - \gamma_3 I_3 - 2g(I_1 I_2 I_3)^{1/2} \cos \psi, \\ \dot{\phi}_3 &= -\frac{|E|}{I_3^{1/2}} \sin(\phi_3 - \phi_0) - g(I_1 I_2 / I_3)^{1/2} \sin \psi,\end{aligned}\tag{4.40}$$

where $E = |E|e^{-i\phi_0}$, $\psi = \phi_1 + \phi_2 - \phi_3$ and

$$\begin{aligned}F_j(t) &= (g\alpha_3^\dagger)^{1/2} \alpha_j \xi_j^\dagger(t) + (g\alpha_3)^{1/2} \alpha_j^\dagger \xi_j(t), \\ f_j(t) &= (g\alpha_3^\dagger)^{1/2} \xi_j^\dagger(t) / (2i\alpha_j^\dagger) - (g\alpha_3)^{1/2} \xi_j(t) / (2i\alpha_j).\end{aligned}\tag{4.41}$$

The above-threshold semiclassical steady-state solution of equation (4.40) would be

$$I_3^0 = \gamma^2 / (4g^2), I^0 = I_1^0 = I_2^0 = \frac{|E|}{g} - \frac{\gamma_3 \gamma}{4g^2}, \phi_0 = 0, \phi_3^0 = \phi_0.$$

To separate out the phase diffusion process, we define $\phi_\pm = \phi_1 \pm \phi_2$ and obtain

the following equations,

$$\begin{aligned}
\dot{I}_1 &= -\gamma I_1 + 2g(I_1 I_2 I_3)^{1/2} \cos \psi + F_1(t), \\
\dot{I}_2 &= -\gamma I_2 + 2g(I_1 I_2 I_3)^{1/2} \cos \psi + F_2(t), \\
\dot{\phi}_+ &= -g[(I_2 I_3 / I_1)^{1/2} + (I_1 I_3 / I_2)^{1/2}] \sin \psi + f_1(t) + f_2(t), \\
\dot{I}_3 &= -2|E|I_3^{1/2} \cos(\phi_3) - \gamma_3 I_3 - 2g(I_1 I_2 I_3)^{1/2} \cos \psi, \\
\dot{\phi}_3 &= \frac{|E|}{I_3^{1/2}} \sin(\phi_3) - g(I_1 I_2 / I_3)^{1/2} \sin \psi, \\
\dot{\phi}_- &= g[(I_1 I_3 / I_2)^{1/2} - (I_2 I_3 / I_1)^{1/2}] \sin \psi + f_1(t) - f_2(t),
\end{aligned} \tag{4.42}$$

We have already taken $\phi_0 = \pi$ here. One can prove that only ϕ_- will experience a phase diffusion process and all other quantities are stable around their corresponding semiclassical steady-state values. We now partially linearize the above equations by defining

$$\begin{aligned}
\Delta I_j &= I_j - I_j^0 (j = 1, 2, 3), \\
\Delta \phi_+ &= \phi_+ - \phi_0, \\
\Delta \phi_3 &= \phi_3 - \phi_0.
\end{aligned} \tag{4.43}$$

We have

$$\begin{aligned}
\Delta \dot{I}_+ &= (4g^2 I^0 / \gamma) \Delta I_3 + F_+^0(t), \\
\Delta \dot{I}_- &= -\gamma \Delta I_- + F_-^0(t), \\
\Delta \dot{I}_3 &= -\frac{\gamma_3}{2} \Delta I_3 - \frac{\gamma}{2} \Delta I_+, \\
\Delta \dot{\phi}_+ &= -\gamma \Delta \phi_+ + \gamma \Delta \phi_3 + f_+^0(t), \\
\Delta \dot{\phi}_3 &= -\frac{\gamma_3}{2} \Delta \phi_3 - (2g^2 I^0 / \gamma) \Delta \phi_+, \\
\dot{\phi}_- &= f_-^0(t),
\end{aligned} \tag{4.44}$$

with $\Delta I_{\pm} = \Delta I_1 \pm \Delta I_2$ and $F_{\pm}^0(t) = F_1(t) \pm F_2(t)$, $f_{\pm}^0(t) = f_1(t) \pm f_2(t)$. The non-zero correlations of these random noise are

$$\begin{aligned}\langle F_+^0(t)F_+^0(t') \rangle &= -\langle F_-^0(t)F_-^0(t') \rangle = 2\gamma I^0 \delta(t-t'), \\ \langle f_-^0(t)f_-^0(t') \rangle &= -\langle f_+^0(t)f_+^0(t') \rangle = (\gamma/2I^0)\delta(t-t').\end{aligned}\quad (4.45)$$

These equations can then be readily solved and the results are the same as in reference [70]. We can then use these results to evaluate the different momenta for the intracavity field. For example,

$$\langle \hat{a}_1(t)\hat{a}_2(t+\tau) \rangle \quad (4.46)$$

$$= \langle \alpha_1(t)\alpha_2(t+\tau) \rangle \quad (4.47)$$

$$= \langle \sqrt{I(t)}_1 e^{-i\phi(t)} \sqrt{I(t+\tau)}_2 e^{-i\phi(t+\tau)} \rangle. \quad (4.48)$$

The linearization gives us

$$\sqrt{I_{1,2}(t)} = (I^0)^{1/2} [1 + (\Delta I_+ \pm \Delta I_-)/(4I^0)], \quad (4.49)$$

$$\phi_{1,2}(t) = \frac{1}{2} [\pi + \Delta\phi_+(t) \pm \phi_-(t)]. \quad (4.50)$$

We have

$$\langle \alpha_1(t)\alpha_2(t+\tau) \rangle \quad (4.51)$$

$$= -\langle [1 + \Delta I_1(t)/(2I^0)] [1 + \Delta I_2(t+\tau)/(2I^0)] \rangle \quad (4.52)$$

$$\times (1 - \frac{1}{2}i\Delta\phi_+(t))(1 - \frac{1}{2}i\Delta\phi_+(t+\tau)) \quad (4.53)$$

$$\times \exp[-\frac{i}{2}(\phi_-(t) - \phi_-(t+\tau))]. \quad (4.54)$$

We note from the boundary condition

$$\alpha_{out}(t) = \sqrt{\gamma}\alpha(t) - \alpha_{in}(t)$$

We simply have

$$\langle \alpha_{out_1}(t) \alpha_{out_2}(t + \tau) \rangle = \gamma \langle \alpha_1(t) \alpha_2(t + \tau) \rangle. \quad (4.55)$$

The Frourie transformation of the time correlation function will give us the spectrum

$$C_{ij}(\omega) = \int_{-\infty}^{\infty} e^{i\omega\tau} \langle \alpha_{out_1}(t) \alpha_{out_2}(t + \tau) \rangle d\tau. \quad (4.56)$$

We will finally get

$$C_{12}(\omega) = -2I^0 L_{\lambda_0} + \frac{1}{8} C_{I_-}(\omega) + \frac{1}{8} C_{\phi_+}(\omega) - \frac{1}{8} C_{I_+}(\omega), \quad (4.57)$$

where

$$L_{\lambda} = \lambda\gamma/(\lambda^2 + \omega^2), \quad (4.58)$$

$$C_{I_-}(\omega) = -L_{(\lambda_0 + \gamma)}, \quad (4.59)$$

$$C_{\phi_+}(\omega) = -\sum_{j=1}^2 \frac{\gamma}{2} \left[\frac{\bar{A}_j^2}{2\bar{\lambda}_j} + \frac{\bar{A}_1 \bar{A}_2}{\bar{\lambda}_1 + \bar{\lambda}_2} \right] L_{\bar{\lambda}_j + \lambda_0}, \quad (4.60)$$

$$C_{I_+}(\omega) = \sum_{j=1}^2 \frac{\gamma}{2} \left[\frac{A_j^2}{2\lambda_j} + \frac{A_1 A_2}{\lambda_1 + \lambda_2} \right] L_{\lambda_j + \lambda_0}, \quad (4.61)$$

where $\lambda_0 = \gamma/(16I^0)$ and

$$\lambda_{1,2} = [\gamma_3 \pm (\gamma_3^2 - 32g^2 I^0)^{1/2}]/4, \quad (4.62)$$

$$\bar{\lambda}_{1,2} = (\gamma/2 + \gamma_3/4) \pm [(\gamma/2 + \gamma_3/4)^2 - 2g|E|]^{1/2}, \quad (4.63)$$

$$A_{1,2} = 1 \mp \frac{\gamma_3}{(\gamma_3^2 - 32g^2 I^0)^{1/2}}, \quad (4.64)$$

$$\bar{A}_{1,2} = 1 \pm \frac{\gamma - \gamma_3/2}{[(\gamma + \gamma_3/2)^2 - 8g|E|]^{1/2}}. \quad (4.65)$$

Similarly we have for

$$S_{ij}(\omega) = \int_{-\infty}^{\infty} e^{i\omega\tau} \langle \alpha_{out_i}^\dagger(t) \alpha_{out_j}(t + \tau) \rangle d\tau, \quad (4.66)$$

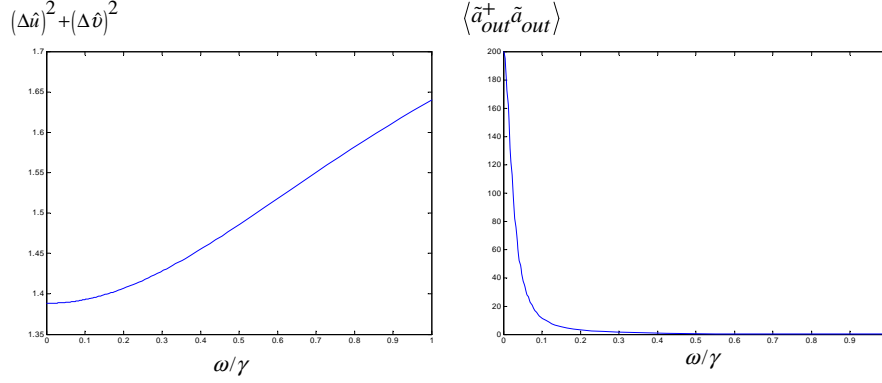


Fig. 19. Dependences of spectrum of the quantum fluctuations of EPR-like operators and intensities on the dimensionless frequency shift ω/γ , for system operating above the threshold $|E| = 2|E|_{thres} = 2\frac{\gamma\gamma_3}{2g}$, with $g/\gamma = 1$ and $\gamma_3/\gamma = 10$.

$$S_{11}(\omega) = S_{22}(\omega) = 2I^0 L_{\lambda_0} + \frac{1}{8}C_{I_-}(\omega) \quad (4.67)$$

$$+ \frac{1}{8}C_{\phi_+}(\omega) + \frac{1}{8}C_{I_+}(\omega). \quad (4.68)$$

We then have for the output field,

$$[(\Delta\hat{u}_{out})^2 + (\Delta\hat{v}_{out})^2]_{\omega} \quad (4.69)$$

$$= 2 + 1/2[C_{I_-}(\omega) + C_{\phi_+}(\omega)] < 2 \quad (4.70)$$

Fig. 19 shows the dependence of the spectrum of quantum fluctuations and the emission rates on the central frequency shift ω/γ . We see the similar behaviour happens here as we have seen for the below-the-threshold case. We then conclude that the steady-state of the output beams of a NOPA system operating above threshold is entangled.

For a summary of this section, we have considered the entanglement in the output field of a nondegenerate optical parametric oscillator for below-threshold and above-threshold cases. We showed that when both input fields are initially in the

vacuum states, we have entanglement in the steady state between the two modes that have opposite frequency shifts from their central frequencies in the output field. We therefore obtain two entangled output beams in this system. These results have potential applications in quantum teleportation and quantum computation.

B. Effects of pump fluctuations on the entanglement of a NOPA system

1. Statistical description of the pump fluctuations

Generally, a non-degenerate optical parametric amplifier (NOPA) under the rotating wave approximation can be described by the following Hamiltonian in the interaction picture:

$$H = \frac{i\hbar\beta}{2}[a_s a_i e^{i\phi} - a_s^\dagger a_i^\dagger e^{-i\phi}]. \quad (4.71)$$

The system is driven by an input laser field and β and ϕ are the amplitude and the phase of this field, respectively. Note that we treat the pump field classically in the parametric approximation and thus ignore the pump depletion here. Two quantized modes, namely the signal (s) and idler (i) modes, are coupled to this pump field. They have either different frequencies or different polarizations with a_s (a_s^\dagger) and a_i (a_i^\dagger) the annihilation (creation) operators associated with these two modes, respectively.

The Heisenberg equations obeyed by the field operators are the following:

$$\begin{aligned} \dot{a}_s &= -\frac{\beta}{2}a_i^\dagger e^{-i\phi}, \\ \dot{a}_s^\dagger &= -\frac{\beta}{2}a_i e^{i\phi}, \\ \dot{a}_i &= -\frac{\beta}{2}a_s^\dagger e^{-i\phi}, \\ \dot{a}_i^\dagger &= -\frac{\beta}{2}a_s e^{i\phi}. \end{aligned} \quad (4.72)$$

It is well known that a laser operating above the threshold generates coherent

field. However, due to the interaction with the environment, there will be phase diffusion and amplitude fluctuation associated with this field. The pump field can therefore be described as

$$\langle b \rangle \equiv \beta e^{-i\phi} = (\beta_0 + \delta\beta) e^{-i\phi(t)}, \quad (4.73)$$

where $\delta\beta$ is the random fluctuation of the amplitude and $\phi(t)$ represents the phase diffusion process.

The amplitude fluctuation in the pump laser can be approximated by an Ornstein-Uhlenbeck stochastic process. The statistics of this process can be described as follows:

$$\begin{aligned} \langle \delta\beta(t) \rangle &= 0, \\ \langle \delta\beta(t) \delta\beta(t') \rangle &= I_A \Gamma e^{-\Gamma|t-t'|}, \end{aligned} \quad (4.74)$$

where I_A is the variance of the amplitude and Γ is the laser linewidth due to amplitude fluctuations.

The phase diffusion of a laser field is a Brownian motion, which can be described by a Wiener-Levy stochastic process,

$$\begin{aligned} \langle \phi(t) \rangle &= 0, \\ \langle \phi(t) \phi(t') \rangle &= D(t + t' - |t - t'|), \end{aligned} \quad (4.75)$$

where D is the diffusion coefficient. The derivative of this diffusion process is a white noise, with

$$\langle \dot{\phi}(t) \dot{\phi}(t') \rangle = 2D \delta(t - t'). \quad (4.76)$$

For a laser operating far above the threshold, the amplitude fluctuation and phase diffusion are independent and thus can be treated separately.

2. Entanglement measures

We again use the sufficient condition for entanglement, which is proposed in ref. [63]. In the present context of non-degenerate parametric oscillator, we need to evaluate the following quantity involving the moments of idler and signal photons:

$$(\Delta\hat{u})^2 + (\Delta\hat{v})^2. \quad (4.77)$$

Here

$$\begin{aligned} \hat{u} &= \hat{x}_s + \hat{x}_i, \\ \hat{v} &= \hat{p}_s - \hat{p}_i \end{aligned} \quad (4.78)$$

and $\hat{x}_j = (a_j + a_j^\dagger)/\sqrt{2}$ and $\hat{p}_j = (a_j - a_j^\dagger)/\sqrt{2}i$ (with $j = s, i$) are the quadrature operators for the signal and idler modes. As shown in [63], a bipartite system is entangled whenever this quantity is less than 2. It has been shown that, for initial vacuum states for signal and idler, the state generated in a NOPA is a continuous variable Gaussian state (in general a mixed state with the consideration of fluctuations) [71] and for such a state, this becomes a necessary and sufficient condition for entanglement.

We also notice that if we substitute the definition of \hat{u} and \hat{v} into equation (4.77), we obtain

$$\begin{aligned} (\Delta\hat{u})^2 + (\Delta\hat{v})^2 &= \langle a_s^\dagger, a_s \rangle + \langle a_s, a_s^\dagger \rangle + \langle a_i^\dagger, a_i \rangle + \langle a_i, a_i^\dagger \rangle + \\ &+ 2(\langle a_s, a_i \rangle + \langle a_s^\dagger, a_i^\dagger \rangle), \end{aligned} \quad (4.79)$$

where we used the notation $\langle a, b \rangle = \langle ab \rangle - \langle a \rangle \langle b \rangle$. If we assume the field modes are initially in vacuum states, the expectation values for all first order momenta of the field will never show up, all we need to evaluate are the following second-order

momenta:

$$\langle a_s^\dagger a_s \rangle, \langle a_i^\dagger a_i \rangle, \langle a_s a_i \rangle, \langle a_s^\dagger a_i^\dagger \rangle. \quad (4.80)$$

3. Phase diffusion upon entanglement generation

It is mainly due to phase fluctuation that a laser operating far above threshold has a natural linewidth. In this section, we address the effect of phase fluctuation upon the entanglement generation of a NOPA system. Far above threshold, the amplitude fluctuations can be effectively ignored. Thus, the driving laser field of the system can be written as

$$\beta e^{-i\phi} \equiv \beta_0 e^{-i\phi(t)}, \quad (4.81)$$

with $\phi(t)$ a Gaussian random variable whose statistics can be described by Eq. (4.75). It follows from Eq. (4.75) and Eq. (4.72) that we obtain (in the compact matrix form)

$$\dot{\hat{\mathbf{O}}} = \mathbf{M}\hat{\mathbf{O}} + i\dot{\phi}(t)\mathbf{N}\hat{\mathbf{O}}, \quad (4.82)$$

where

$$\hat{\mathbf{O}} = \begin{pmatrix} a_s a_s^\dagger + a_i^\dagger a_i \\ a_i a_i^\dagger + a_s^\dagger a_s \\ a_s a_i e^{i\phi(t)} \\ a_s^\dagger a_i^\dagger e^{-i\phi(t)} \end{pmatrix} \quad (4.83)$$

and

$$\mathbf{M} = \begin{pmatrix} 0 & 0 & -\beta_0 & -\beta_0 \\ 0 & 0 & -\beta_0 & -\beta_0 \\ -\frac{\beta_0}{2} & 0 & 0 & 0 \\ 0 & -\frac{\beta_0}{2} & 0 & 0 \end{pmatrix}, \quad \mathbf{N} = \begin{pmatrix} 0 & 0 & 0 & 0 \\ 0 & 0 & 0 & 0 \\ 0 & 0 & 1 & 0 \\ 0 & 0 & 0 & -1 \end{pmatrix}. \quad (4.84)$$

For the random phase given by a Wiener-Levy process, we obtain the following equation:

$$\langle \dot{\hat{\mathbf{O}}} \rangle = [\mathbf{M} - D\mathbf{N}^2] \langle \hat{\mathbf{O}} \rangle. \quad (4.85)$$

We consider the case when both modes are initially in vacuum states, that is

$$\langle \dot{\hat{\mathbf{O}}}(0) \rangle = \begin{pmatrix} 1 \\ 1 \\ 0 \\ 0 \end{pmatrix}. \quad (4.86)$$

Equation (4.85) can then be solved in a straightforward way. The results for the concerned quantities are

$$\begin{aligned} \langle a_s a_s^\dagger + a_s^\dagger a_s + a_i^\dagger a_i + a_i a_i^\dagger \rangle(t) = \\ \frac{2e^{-\frac{1}{2}Dt}}{\beta} [D \sinh(\frac{1}{2}\beta t) + \beta \cosh(\frac{1}{2}\beta t)], \end{aligned} \quad (4.87)$$

where $\beta = \sqrt{D^2 + 4\beta_0^2}$.

We now need to evaluate the stochastic average of $\langle a_s a_i \rangle$. From the Heisenberg equation (4.72) with the phase fluctuations, we obtain the same form of matrix equations as Eqs. (4.82) with the following substitutions:

$$\hat{\mathbf{O}} = \begin{pmatrix} a_s a_i \\ (a_i^\dagger a_i + a_s a_s^\dagger) e^{-i\phi(t)} \\ a_s^\dagger a_i^\dagger e^{-2i\phi(t)} \end{pmatrix}, \quad (4.88)$$

with

$$\mathbf{M} = \begin{pmatrix} 0 & \frac{-\beta_0}{2} & 0 \\ -\beta_0 & 0 & -\beta_0 \\ 0 & -\frac{\beta_0}{2} & 0 \end{pmatrix}, \quad \mathbf{N} = \begin{pmatrix} 0 & 0 & 0 \\ 0 & -1 & 0 \\ 0 & 0 & -2 \end{pmatrix}. \quad (4.89)$$

The expectation values of $\hat{\mathbf{O}}$ satisfy the same form of equations (4.85) with suitable substitutions. This equation can be solved straightforwardly by using, for example, the Laplace Transforms. With the initial condition of

$$\langle \dot{\hat{\mathbf{O}}}(0) \rangle = \begin{pmatrix} 0 \\ 1 \\ 0 \end{pmatrix}, \quad (4.90)$$

we obtain

$$\langle a_s a_i \rangle(t) = - \sum_{i,j,k, i \neq j \neq k} e^{-\lambda_i t} \frac{\beta_0(\lambda_i + 4D)}{2(\lambda_i - \lambda_j)(\lambda_i - \lambda_k)}, \quad (4.91)$$

where λ_i 's are the roots of the following Cubic equation:

$$\lambda^3 + 5D\lambda^2 + (4D^2 - \beta_0^2)\lambda - 2\beta_0 D = 0.$$

The resulting solution is then

$$\begin{aligned} [(\Delta \hat{u})^2 + (\Delta \hat{v})^2](t) &= 2\left\{ \frac{e^{-\frac{1}{2}Dt}}{2\beta_0} [D \sinh(\beta_0 t) + 2\beta_0 \cosh(\beta_0 t)] \right. \\ &\quad \left. - \sum_{i,j,k, i \neq j \neq k} e^{-\lambda_i t} \frac{\beta_0(\lambda_i + 4D)}{2(\lambda_i - \lambda_j)(\lambda_i - \lambda_k)} \right\}. \end{aligned} \quad (4.92)$$

Fig. 20 shows the time evolution of $(\Delta \hat{u})^2 + (\Delta \hat{v})^2$ with various diffusion constants and noise-intensity ratios D/β_0 . We have chosen $\beta_0 t$ as our dimensionless time scale. We see that from this figure, the entanglement will be finally eliminated due to the phase fluctuations. This elimination becomes faster when the phase fluctuations are strong.

4. Effect of amplitude fluctuations

Although we expect that the effect of amplitude fluctuations upon entanglement generation are much weaker than the ones due to the phase fluctuations, it is still

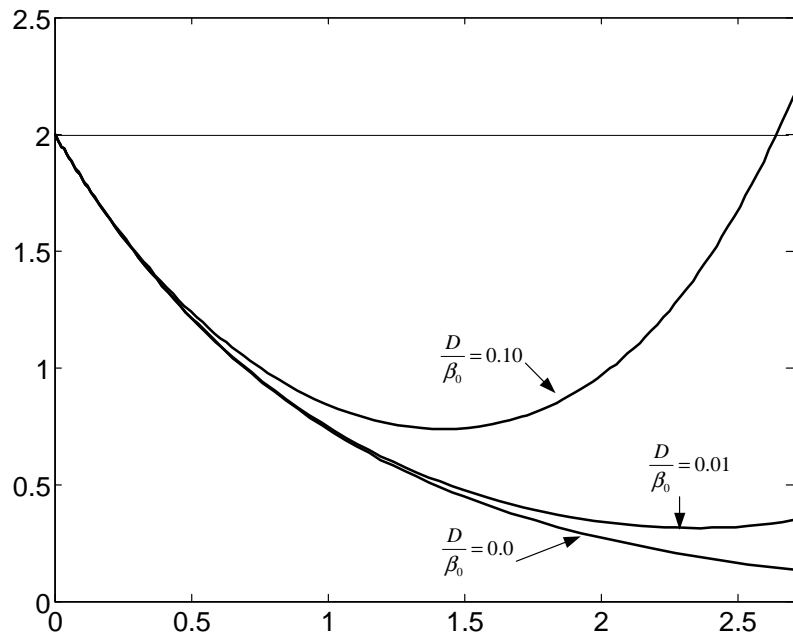


Fig. 20. $(\Delta \hat{u})^2 + (\Delta \hat{v})^2$ vs $\beta_0 t$ for $D/\beta_0 = 0.0, 0.01$, and 0.10

worthwhile to look at this problem. For this purpose we set $\phi = 0$ and assume no phase diffusions here. On substituting $\beta = \beta_0 + \delta\beta(t)$ in the Heisenberg equations (4.72), we find that the various moments needed for our entanglement measurement form the following closed set of equations (we again write them here in the compact matrix form):

$$\dot{\hat{\mathbf{O}}} = \mathbf{M}\hat{\mathbf{O}} + i\delta\beta(t)\mathbf{N}\hat{\mathbf{O}}, \quad (4.93)$$

where

$$\hat{\mathbf{O}} = \begin{pmatrix} a_s^\dagger a_s + a_s a_s^\dagger \\ a_i^\dagger a_i + a_i a_i^\dagger \\ a_s a_i + a_s^\dagger a_i^\dagger \end{pmatrix} \quad (4.94)$$

and

$$\mathbf{M} = \begin{pmatrix} 0 & 0 & -\beta_0 \\ 0 & 0 & -\beta_0 \\ -\frac{\beta_0}{2} & -\frac{\beta_0}{2} & 0 \end{pmatrix}, \quad \mathbf{N} = i \begin{pmatrix} 0 & 0 & 1 \\ 0 & 0 & 1 \\ \frac{1}{2} & \frac{1}{2} & 0 \end{pmatrix}. \quad (4.95)$$

The matrices \mathbf{M} and \mathbf{N} commute. It then follows from the characteristics of a Gaussian stochastic process, that the expectation value of $\hat{\mathbf{O}}$ satisfies the following equation:

$$\langle \dot{\hat{\mathbf{O}}} \rangle = [\mathbf{M} - \mathbf{N}^2 g(t)] \langle \hat{\mathbf{O}} \rangle, \quad (4.96)$$

where

$$g(t) = I_A(1 - e^{-\Gamma t}). \quad (4.97)$$

For initial vacuum states for the signal and idler modes, this equation can be solved analytically. The resulting solution for the entanglement measure is:

$$(\Delta \hat{u})^2 + (\Delta \hat{v})^2 = 2e^{f(t) - \beta_0 t}, \quad (4.98)$$

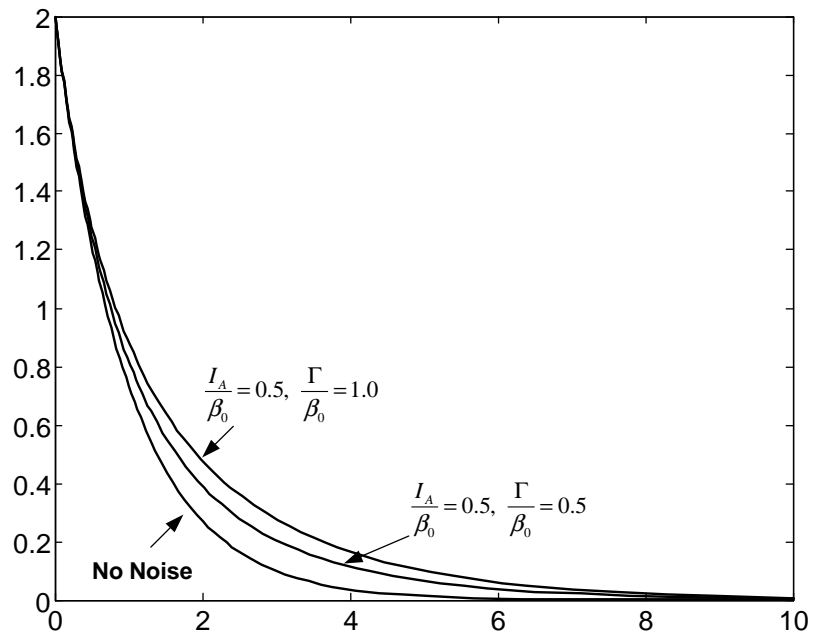


Fig. 21. $(\Delta \hat{u})^2 + (\Delta \hat{v})^2$ vs $\beta_0 t$ for no noise; $I_A/\beta_0 = 0.5$, $\Gamma/\beta_0 = 0.5$; $I_A/\beta_0 = 0.5$, $\Gamma/\beta_0 = 1.0$.

where $f(t) = \int_0^t g(t')dt' = I_A t + I_A(e^{-\Gamma t} - 1)/\Gamma$. In Fig. (21), we show our results for various conditions of the driving amplitude fluctuations. For a typical laser system, we have $I_A < \beta_0$ and we see that the amplitude fluctuation only slows the progress of the system going into an entangled state. The maximumly entangled state will always be obtained when the time lapses to infinity. This result confirms our expectations.

In this section, we have investigated the effect of amplitude and phase fluctuations of the pump field on the entanglement characteristics of the idler and signal fields in a NOPA system. The NOPA system has long been known to generate two-mode squeezing. The generation of macroscopic entangled states through parametric down conversion systems has also been proposed and experimentally implemented [36, 72, 73, 51]. Here we have shown that the effect of pump phase and amplitude fluctuations is to reduce the entanglement. We conclude that, using a laser with controllable phase and amplitude fluctuations, the results obtained in this paper can be verified by an experiment such as the one discussed in [36].

CHAPTER V

SUMMARY

In summary, we have studied entanglement generation in thermal states. We found that entanglement could be generated between an atom and a thermal field if the differential temperature of these two interacting systems is sufficiently large. Entanglement can even be generated when the initial temperature of the thermal field is quite high. We also addressed the problem of entanglement generation between two thermal fields. It turns out that atomic coherence plays an essential role in this entanglement generation. Two important quantum concepts, namely coherence and entanglement, are shown to be closely related in this case. We also proposed a new entanglement amplifier base on a two-photon correlated emission laser system and studied the entanglement generation and the effects of pumping fluctuations upon the entanglement generation in this system. We performed an input-output calculation for a NOPA system and studied the pumping fluctuation effects in this system.

REFERENCES

- [1] M. O. Scully, M. S. Zubairy, G. S. Agarwal and H. Walther, *Science* **299**, 862 (2003).
- [2] M. O. Scully, *Phys. Rev. Lett.* **55**, 2802 (1985).
- [3] M. O. Scully and M. S. Zubairy, *Phys. Rev. A* **35**, 752 (1987).
- [4] J. Bergou, M. Orszag, and M. O. Scully, *Phys. Rev. A* **38**, 768 (1988).
- [5] J. Krause and M. O. Scully, *Phys. Rev. A* **36**, 1771 (1987).
- [6] M. O. Scully, K. Wódkiewicz, M. S. Zubairy, J. Bergou, N. Lu, and Meyerter Vehn, *Phys. Rev. Lett.* **60**, 1832 (1988).
- [7] M. Ohtsu and K.-Y. Liou, *Appl. Phys. Lett.* **52**, 10 (1988).
- [8] M. O. Scully, *Phys. Rev. Lett.* **67**, 1855 (1991).
- [9] G. Alzetta, A. Gozzini, L. Moi, and G. Orriols, *Nuovo Cimento* **36B**, 5 (1976).
- [10] S. E. Harris, J. E. Field, and A. Imamoglu, *Phys. Rev. Lett.* **64**, 1107 (1990).
- [11] A. Javan, *Phys. Rev.* **107**, 1579 (1956).
- [12] O. Kocharovskaya and Ya. I. Khanin, *Pis'ma Zh. Eksp. Teor. Fiz.* **48**, 581 (1988)(*JETP Lett.* **48**, 630 (1988)).
- [13] M. O. Scully, S.-Y. Zhu, and A. Gavrielides, *Phys. Rev. Lett.* **62**, 2813 (1989).
- [14] A. Einstein, B. Podolsky, and N. Rosen, *Phys. Rev.* **47**, 777(1935).
- [15] E. Schrödinger, *Proc. of the Cambridge Philosophical Society*, **31**, 555 (1935).

- [16] D. Bohm, *Quantum Theory* (Prentice-Hall, Englewood Cliffs, NJ, 1951).
- [17] J. S. Bell, *Physics* **1**, 195(1964); *Rev. Mod. Phys.* **38**, 447(1966).
- [18] E. Hagley, X. Maitre, G. Nogues, C. Wunderlich, M. Brune, J. M. Raimond, and S. Haroche, *Phys. Rev. Lett.* **79**, 1(1997).
- [19] Q. A. Turchette, C. S. Wood, B. E. King, C. J. Myatt, D. Leibfried, W. M. Itano, C. Monroe, and D. J. Wineland, *Phys. Rev. Lett.* **81**, 3631(1998).
- [20] K. Molmer and A. Sorensen, *Phys. Rev. Lett.* **82**, 1835(1999).
- [21] C. A. Sackett, D. Kielpinski, B. E. King, C. Langer, V. Meyer, C. J. Myatt, M. Rowe, Q. A. Turchette, W. M. Itano, D. J. Wineland, and C. Monroe, *Nature* **404**, 256(2000).
- [22] L. M. Duan, J. I. Cirac, P. Zoller and E. S. Polzik, *Phys. Rev. Lett.* **85**, 5643(2000).
- [23] B. Julsgaard, A. Kozhekin and E. S. Polzik, *Nature* **413**, 400(2001).
- [24] A. Rauschenbeutel, P. Bertet, S. Osnaghi, G. Nogues, M. Brune, J. M. Raimond, and S. Haroche, *Phys. Rev. A* **64**, 050301(2001).
- [25] S. J. Freedman and J. F. Clauser, *Phys. Rev. Lett.* **28**, 938(1972).
- [26] J. F. Clauser, *Phys. Rev. Lett.* **36**, 1223(1975).
- [27] E. S. Fry and R. C. Thompson, *Phys. Rev. Lett.* **37**, 465(1976).
- [28] Z. Y. Ou and L. Mandel, *Phys. Rev. Lett.* **61**, 50(1988).
- [29] P. G. Kwiat, K. Mattle, H. Weinfurter, and A. Zeilinger, *Phys. Rev. Lett.* **75**, 4337(1995).

- [30] D. Bouwmeester, J.-W Pan, M. Daniell, H. Weinfurter, and A. Zeilinger, Phys. Rev. Lett. **82**, 1345(1998).
- [31] J.-W. Pan, M. Daniell, S. Gasparoni, G. Weihs, and A. Zeilinger, Phys. Rev. Lett. **86**, 4435(2001).
- [32] Z. Zhao, Y.-A. Chen, A.-N. Zhang, T. Yang, H. J. Briegel, and J. W. Pan, Nature **430**, 54(2004).
- [33] K. Tsujino, H. F. Hofmann, S. Takeuchi, and K. Sasaki, Phys. Rev. Lett. **92**, 153602(2004).
- [34] H. S. Eisenberg, G. Khoury, G. A. Durkin, C. Simon, and D. Bouwmeester, Phys. Rev. Lett. **93**, 193901(2004).
- [35] S. L. Braunstein and P. van Loock, Quant-ph/0410100.
- [36] Y. Zhang, H. Wang, X. Y. Li, J. T. Jing, C. D. Xie, and K. C. Peng, Phys. Rev. A **62**, 023813(2000).
- [37] A. Barenco, D. Deutsch, A. Ekert, and R. Jozsa, Phys. Rev. Lett. **74**, 4083(1995).
- [38] C. H. Bennett and S. J. Wiesner, Phys. Rev. Lett. **69**, 2881(1992).
- [39] A. K. Ekert, Phys. Rev. Lett. **67**, 6961(1991).
- [40] C. H. Bennett, G. Brassard, C. Crepeau, R. Jozsa, A. Peres and W. K. Wootters, Phys. Rev. Lett. **70**, 1895(1993).
- [41] D. Bouwmeester, J.-W. Pan, K. Mattle, M. Eibl, H. Weinfurter, and A. Zeilinger, Nature **390**, 6660, 575-579 (1997).

- [42] M. Riebe, H. Häffner, C. F. Roos, W. Hänsel, J. Benhelm, G. P. T. Lancaster, T. W. Körber, C. Becher, F. Schmidt-Kaler, D. F. V. James, R. Blatt, *Nature* **429**, 734 - 737 (2004).
- [43] V. Vedral, M. B. Plenio, M. A. Rippin, and P. L. Knight, *Phys. Rev. Lett.* **78**, 2275 (1997).
- [44] V. Vedral and M. B. Plenio, *Phys. Rev. A* **57**, 1619 (1998).
- [45] C. H. Bennett, D. P. DiVincenzo, J. A. Smolin, and W. K. Wootters, *Phys. Rev. A* **54**, 3824 (1996).
- [46] W. K. Wootters, *Phys. Rev. Lett.* **80**, 2245 (1998).
- [47] S. Bose, I. Fuentes-Guridi, P. L. Knight, and V. Vedral, *Phys. Rev. Lett.* **87**, 050401 (2001).
- [48] E. T. Jaynes and F. W. Cummings, *Proc. IEEE* **51**, 89 (1963).
- [49] A. Peres, *Phys. Rev. Lett.* **77**, 1413 (1996).
- [50] M. Horodecki, P. Horodecki, and R. Horodecki, *Phys. Lett. A* **223**, 1 (1996).
- [51] R. Simon, *Phys. Rev. Lett.* **84**, 2726(2000).
- [52] M. O. Scully and M. S. Zubairy, *Quantum Optics*, (Cambridge Press, London 1997).
- [53] M. S. Kim, J. Lee, D. Ahn, and P. L. Knight, *Phys. Rev. A* **65**, 040101(R) (2002).
- [54] H. Kühn, D.-G. Welsch, and W. Vogel, *Phys. Rev. A* **51**, 4240 (1995); M. G. Raymer, D. F. McAlister, and U. Leonhardt, *ibid.* **54**, 2397 (1996); M. S. Kim and G. S. Agarwal, *ibid.* **59**, 3044 (1999); G. M. D'Ariano, M. F. Sacchi, and P.

- Kumar, *ibid.* **61**, 013806 (1999); J. Fiurasek, *ibid.* **63**, 033806 (2001); M. Ahmad, S. Qamar, and M. S. Zubairy, *ibid.* **67**, 043815 (2003).
- [55] M. Ikram and M.S. Zubairy, *Phys. Rev. A* **65**, 044305 (2002).
- [56] M. S. Zubairy, in *Quantum Limits to the Second Law: First International Conference*, edited by D. P. Sheehan, (AIP Conference Proceedings, San Diego, California, 2002) pp. 92-97.
- [57] J. Lee and M. S. Kim, *Phys. Rev. Lett.* **84**, 4236 (2000).
- [58] N. A. Ansari, J. Gea-Banacloche, and M. S. Zubairy, *Phys. Rev. A* **41**, 5179 (1990).
- [59] J. McKeever, A. Boca, A. D. Boozer, J. R. Buck and H. J. Kimble, *Nature* **425**, 268 (2003).
- [60] C. H. van der Wal, M. D. Eisaman, A. André, R. L. Walsworth, D. F. Phillips, A. S. Zibrov and M. D. Lukin, *Science* **301**, 196 (2003).
- [61] M. O. Scully and M. S. Zubairy, *Opt. Commun.* **66**, 303 (1988).
- [62] C. A. Blockley and D. F. Walls, *Phys. Rev. A* **43**, 5049 (1991).
- [63] L. M. Duan, G. Giedke, J. I. Cirac and P. Zoller, *Phys. Rev. Lett.* **84**, 2722 (2000).
- [64] D. Meschede, H. Walther, and G. Muller, *Phys. Rev. Lett.* **54**, 551 (1985); G. Raqithel, C. Wagner, H. Walther, L. M. Narducci, and M. O. Scully, in *Advances in Atomic, Molecular, and Optical Physics*, edited by P. Berman (Academic, New York 1994), Supp. 2, p. 57.

- [65] J. M. Raimond, M. Brune, and S. Haroche, *Rev. Mod. Phys.* **73**, 565 (2001).
- [66] Mark Hillery and M. S. Zubairy, *Phys. Rev. Lett.* **96**, 050503 (2006).
- [67] M. O. Scully and M. S. Zubairy, *Phys. Rev. A* **38**, 754 (1998).
- [68] H. Xiong, M. O. Scully and M. S. Zubairy, *Phys. Rev. Lett.* **94**, 023902 (2005).
- [69] M. J. Collett and C. W. Gardiner, *Phys. Rev. A* **30**, 1386 (1984).
- [70] M. D. Reid and P. D. Drummond, *Phys. Rev. A* **40**, 4493 (1989).
- [71] H. T. Tan, S. Y. Zhu, and M. S. Zubairy, *Phys. Rev. A* **72**, 022305 (2005).
- [72] Ch. Silberhorn, P. K. Lam, O. Weiß, F. König, N. Korolkova and G. Leuchs, *Phys. Rev. Lett.* **86**, 4267 (2001).
- [73] W. P. Bowen, N. Treps, R. Schnabel, and P. K. Lam, *Phys. Rev. Lett.* **89**, 253601 (2002).

VITA

Han Xiong

- Physics Dept, c/o Dr. M. Suhail Zubairy
Texas A&M M.S.4242
College Station, Texas 77843-4242

Education:

- Texas A&M University, College Station, Texas
Ph.D. in Theoretical Physics-Quantum Optics GPA: 3.8/4.0 May 2006
Co-advisors: Dr. M. Suhail Zubairy, Dr. Marlan O. Scully
- Institute of Physics, Chinese Academy of Sciences, Beijing, China
M. S. in Solid-State Physics GPA: 3.9/4.0 July 2000
Advisor: Dr. Yushu Yao
- Peking (Beijing) University, Beijing, China
B. S. in Physics GPR: 3.9/4.0 July 1997

Selected Publications:

- Correlated Spontaneous Emission Laser as an Entanglement Amplifier, Han Xiong, Marlan O. Scully and M. Suhail Zubairy, Phys. Rev. Lett. **94**, 023601(2005).
- Coherence Induced Entanglement, Fuli Li, Han Xiong and M. Suhail Zubairy, Phys. Rev. A **72**, 010303(Rapid Communications), (2005).